Available online at www.CivileJournal.org

Civil Engineering Journal

(E-ISSN: 2476-3055; ISSN: 2676-6957)

Vol. 11, No. 08, August, 2025

Statistical Analyses of the Euphrates River Entry and Hydrological Drought Assessment (SDI)

Zainab Hussein [1*], Saleh I. Khassaf [1]

[1] *Department of Civil Engineering, University of Basrah, Basrah, 61001, Iraq.*

Received 14 May 2025; Revised 11 July 2025; Accepted 20 July 2025; Published 01 August 2025

Abstract

The Euphrates River, a vital water resource in Iraq, has seen a marked decline in flow over the past two decades due to climate change and upstream interventions. The aim of this study is to investigate the impacts of changing rainfall patterns and temperature on the river's water balance, flow regime, and drought index. Results show an annual rainfall decline of 0.15 mm, while maximum and minimum temperatures increased annually by 0.086°C and 0.066°C, respectively, according to the Mann-Kendall trend and Sen's slope tests. Monthly rainfall generally decreased, except for slight increases in April (0.32 mm) and October (0.018 mm). July 2017 and August 2003 saw peak temperatures of 45.1°C, while January 2008 recorded a minimum of -1.8°C. The box-and-whisker plot revealed high rainfall variability in November and February. River flow dropped by 41%, mainly due to the Turkish GAP project and climate impacts. HEC-DSS software analyzed flow duration over 32 years, and Pearson's correlation showed low associations between flow rate and temperature (-0.36) and rainfall (0.29). The Drinc program was utilized to calculate the Standardized Drought Index, which identified that the water year 1987–1988 was very wet, while it detected severe droughts in 2014–2015 and 2021–2022. Overall, climate change and upstream dam construction have significantly reduced Euphrates River discharges, intensifying drought conditions in the region. The long-term changes in precipitation and air temperature in the study area support the observed streamflow trends. The findings of this study demonstrate that a cooperative approach to international water management between the riparian states is crucial.

Keywords: Euphrates River; Drought Index; Temperature; Climate; Drinc.

1. Introduction

The Middle East has been struggling with water scarcity, particularly recently, due to inadequate water management amid population growth, agricultural expansion, urban and industrial development, and climate change. These factors have collectively intensified the demand for freshwater, posing a significant threat to both water and food security in the region. By 2030, per capita water availability is projected to decline below the critical threshold of 500 cubic meters [1]. Climate change plays a substantial role in global water scarcity by altering weather patterns, which include increased temperatures and changes in precipitation, leading to natural disasters such as floods and droughts of varying durations and intensities. Currently, these climatic changes are largely attributed to human activities, particularly global warming, which results from population growth and increased fossil fuel consumption, leading to greenhouse gas emissions. The atmospheric concentration of carbon dioxide has reached unprecedented levels compared to the past 500,000 years, showing a rapid and significant rise, which has caused annual temperatures to exceed those recorded in the previous millennium. The Intergovernmental Panel on Climate Change (IPCC) has concluded that there is a likelihood of the Earth's temperature increasing by 1.5 to 2 degrees Celsius between 2020 and 2040. Climate change has significantly

* Corresponding author: engpg.zeinab.hussein@uobasrah.edu.iq

http://dx.doi.org/10.28991/CEJ-2025-011-08-04

worsened water scarcity in arid and semi-arid regions, particularly affecting Arab nations. Approximately 362 million people are currently facing water scarcity [2], threatening water security and national security in the region, compromising water sustainability, and negatively impacting food security, energy, and the environment. Iraq's hot, dry climate is characterized by long, very warm summers and short, cool winters. The climate is influenced by Iraq's location between the subtropical aridity of the Arabian desert areas and the Arabian Gulf's subtropical humidity, which makes it especially susceptible to temperature variations and droughts. This vulnerability has ranked it as the fifth most affected country globally by these changes, facing significant challenges like decreased rainfall, increased temperatures, drought, desertification, lost plant cover, and elevated salinity levels [3].

Iraq has significant water resources, which include the Tigris and Euphrates rivers, as well as many lakes and other water bodies, making it one of the nations rich in water resources. The Euphrates River is a principal river in Iraq and the second longest in the Arab world, measuring around 2,940 kilometers, with 39.5% of its length in Iraq. The Euphrates River serves as the primary water source for the urban, agricultural, and industrial sectors in western Iraq, the Euphrates region, and southern Iraq. The Euphrates River is heavily used by riparian states, which have developed various infrastructures along its banks. This includes Turkey's Cape Anatolia Project (CAP) and several dams in Syria, both of which adversely affect the quantity and quality of water flowing into Iraq. The river experiences significant variations in flow on both monthly and annual scales, influenced by the operational policies of upstream countries and the impacts of climate change. The mean annual discharge of the Euphrates River from 1933 to 1972 was 30.26 billion cubic meters before the initiation of the Southeastern Anatolia Project. This average subsequently decreased to 26.23 billion cubic meters between 1976 and 1989, which can be attributed to the filling of the Keban Dam in Turkey and the Tabqa Dam in Syria between 1973 and 1977. The annual inflow continued to decline, reaching 15.11 billion cubic meters from 1999 to 2021, a reduction linked to the Atatürk Dam's filling period from 1992 to 1995. Under natural conditions, the discharge of the Euphrates occurs in three distinct phases: elevated flow during the spring flood season, from February to June; reduced discharge during the low water season, from July to September; and intermediate discharge from autumn to winter, from October to January.

Al-Muhyi et al. [4] examined the monthly and annual trends in mean, maximum, and minimum temperatures and humidity in Basra City from 1941 to 2013. The findings indicated an increase in monthly and annual temperatures alongside a decrease in humidity; the annual mean temperature in Basra Province is anticipated to reach 7.6°C by 2100. Arvind et al. [5] analyzed annual rainfall in Musiri town over 30 years using plotting position and probabilistic methods to ascertain the return period. An analysis of seasonal rainfall was conducted using multiple statistical characteristics, including the arithmetic mean, standard deviation, coefficient of variation, and coefficient of skewness. Zaghloul et al. [6] used the Mann-Kendall test and Sen's slope at varying significance levels to assess long-term trends in water flow within the Athabasca River Basin (ARB) and Peace River Basin (PRB), along with long-term trends in temperature and precipitation from 1956 to 2020. This analysis aimed to elucidate the correlation between climate change and water flow, emphasizing the need to investigate the impacts of human activities and land cover on water availability, as well as the relationship between surface water and groundwater across the different subregions of the ARB and PRB. Additionally, it is recommended to conduct the same investigation in the next five to ten years to determine if the observed increase in water flow continues. Rao et al. [7] used the Mann-Kendall test and the Theil-Sen estimator to detect and quantify trends in precipitation data in the Chinta Palle region to understand the impact of climate change on precipitation trends. Linear regression analysis reveals an annual rainfall increase of 2.13 mm per year. The Rainfall Anomaly Index (RAI) and the Standard Precipitation Index (SPI) are used to assess the frequency and severity of droughts.

Minh et al. [8] looked at how the Vietnamese Mekong Delta (VMD) precipitation patterns changed between 1978 and 2022 to understand how these patterns differed in inland and coastal areas. Several statistical techniques, such as the Mann-Kendall test, the sequential Mann-Kendall test, and advanced trend analysis, are employed to investigate rainfall patterns. Muhammad & Obead [9] utilized the Standard Precipitation Index (SPI) and the Standard Precipitation and Evapotranspiration Index (SPEI) to evaluate drought conditions in the Euphrates River basin, namely in Hilla, Karbala, Najaf, and Diwaniyah. The investigation identified severe droughts in Samawah in 2012 and Diwaniyah in 1999, with severity levels of -2.8957 in SPI-12 and SPEI-12, respectively. Leone and Oculi [10] utilized gene expression programming (GEP) in conjunction with the Mann-Kendall (MK) trend analysis and Sen's slope tests to evaluate long-term fluctuations and trends in precipitation and air temperature in St. Lucia from 1990 to 2020. The findings indicate an absence of significant trends in precipitation during the past three decades. The GEP analysis forecasts likely drought conditions marked by reduced rainfall over the next decade, suggesting a change in precipitation patterns, while the island's average temperature is expected to increase by 0.032°C per year. Abubakar et al. [11] Analyzed rainfall and temperature data utilizing linear regression, standard deviation, and second-order polynomial curve fitting; while Cramer's test was applied to evaluate decadal trends in these variables, the student's t-test was employed to assess the comparative impacts of the periods 1961-1990 and 1991-2020 on the observed variations in rainfall and temperature. Cramer's and T-test results demonstrated a significant increase in monthly and annual rainfall and temperature over the past three decades.

Drought is an extended arid phase in the natural climatic cycle that may take place globally [12]. It is a gradual disaster marked by insufficient precipitation, leading to a water deficit. Drought can significantly affect health, agriculture, the economy, energy, and the environment. Climate change is increasing the frequency and severity of droughts in many regions worldwide [13]. Drought is categorized into four types: meteorological, hydrological, agricultural, and socioeconomic. The initial three methodologies assess drought as a physical phenomenon, while the socioeconomic type addresses drought in terms of supply and demand [14]. Drought monitoring can utilize several indicators, including the Standardized Precipitation Index (SPI), the Standardized Precipitation-Evapotranspiration Index (SPEI), the Surface Water Supply Index (SWSI), the Aggregate Drought Index (ADI), and the Streamflow Drought Index (SDI) over multiple time scales. Drought constitutes a significant concern in Iraq, with other hydrological hazards such as floods, sandstorms, and rainstorms [15] indicating this region's prospective challenges if such extreme weather phenomena persist. Drought and floods have seriously impacted agricultural regions and livelihoods in Iraq throughout the initial decade of the 21st century, as the nation experienced persistent drought occurrences that have intensified in recent decades. The intense drought that impacted the nation from 2007 to 2009 broke around 40% of agricultural land [16] and drove 20,000 rural inhabitants to relocate in pursuit of adequate drinking water and more viable livelihoods. The reduction in precipitation and water flow, coupled with the increased evaporation rate resulting from regional global warming, will result in diminished soil moisture and insufficient groundwater recharge. These alterations will subsequently impact both rain-fed and irrigated agriculture in the Tigris-Euphrates basin [17]. If no action is taken to implement essential adaptations to climate change, given the rising temperatures and declining precipitation, this will contribute to a shortage between water supply and demand, leading to a water shortfall that exceeds 11 billion cubic meters by 2035 [18].

Many studies have been undertaken to assess drought severity, frequency, and duration using various indicators. Nasir & Hamdan [19] employed standardized precipitation indexes (SPI6 and SPI12) to analyze drought conditions in Iraq across 24 meteorological stations from 1950 to 2016. Iraq has seen both short-term and long-term droughts, especially in the recent decades (1997–2016), attributed to climate change and global warming. Moreover, Nedham & Hassan [20] assessed drought in Iraq at monitoring stations (Mosul, Baghdad, Rutba, and Basrah) utilizing three indices: the Standardized Precipitation Index (SPI), the Percentage Anomaly of Precipitation (PAP), and the Z-Score Index (ZSI) over six months across two distinct periods, from 1970 to 2015 and projected from 2016 to 2050 under the RCP4.5 scenario. The findings indicate that the PPA is the most efficacious metric for drought evaluation during the initial period (1970–2015); in contrast, the ZSI is the most suitable for the later timeframe (2016–2050). Similarly, Tareke & Awoke [21] assessed the hydrological drought utilizing two indicators, SDI and M1SWSI, over eight river basins in Ethiopia from 1973 to 2014. The SDI provides a more comprehensive and realistic depiction of severe drought cases and their frequency, in contrast to the M1SWSI, which produced inaccurate results due to accumulated hydrological inputs. The 1980s experienced the most severe drought conditions.

Moreover, Dare et al. [22] evaluated the climatic and hydrological drought of the Kaduna River catchment area from 1967 to 2001 using SPI, RDI, and SDI indices with *DrinC* software. The drought severity indicated 33% and 37% drought conditions over the research period. The data reveals that normal conditions were more common than drought situations. Only one instance of extreme drought conditions occurred during the 34-year study period, with a recurrence interval of one year. Likewise, Al-Khafaji and Al-Ameri [23] used *DrinC* software to analyze drought conditions at meteorological and streamflow stations near Mosul Dam in northern Iraq from 1979 to 2013, employing the Reconnaissance Drought Index (RDI), Standardized Precipitation Index (SPI), and the Streamflow Drought Index (SDI). The RDI revealed a higher frequency of arid periods relative to the other two indices. Al-Muhyi et al. [24] Employed Linear Regression Equations, Coefficients of Determination (R^2), Precipitation Concentration Index (PCI), and Rainfall Variability Index (RVI) to evaluate the influence of climate change on the spatial and temporal distribution of precipitation in Iraq. Dakhil et al. [25] employed the Normalized Difference Vegetation Index (NDVI) and the Vegetation Condition Index (VCI) to assess the drought conditions in the northern part of Wasit province, Iraq, from 1993 to 2023 by remote sensing technologies. NDVI studies demonstrated that vegetation cover peaked in 1993 and 1998, dropping to its nadir in 2023, whereas VCI results suggested severe drought conditions from 2003 to 2023. da Silva et al. [26] used the Standardized Precipitation-Evapotranspiration Index (SPEI) to assess drought conditions in the Semear Digital Centre's Agrotechnological Districts (DATs) from 2000 to 2024. Moderate and minor droughts were the most commonly seen category in the DATs.

The majority of the above studies focus on understanding climate patterns and their variations, as well as developing predictive models through statistical analyses of precipitation and temperature. The importance of using drought indicators to assess drought patterns, severity, probability of occurrence, and impacts, especially in regions facing water scarcity. These evaluations furnish essential information to decision-makers across multiple sectors, including agriculture, water resource management, and disaster preparedness.

This study aims to look at the yearly changes in important weather data along the Euphrates River from 1991 to 2022, such as rainfall and the maximum and minimum temperatures, to understand climate changes using the Mann–Kendall trend model (MKTM). Sen's slope estimator (SSE) and the linear regression approach were employed to

evaluate the monthly trends of maximum temperature (Tmax), minimum temperature (Tmin), and precipitation over 32 years. The box-and-whisker plot illustrates the monthly variation of rainfall, while statistical parameters were employed to assess the annual variability of rainfall by segmenting the time series into four periods to yield more precise results. The U.S. Army Corps of Engineers Hydrologic Engineering Center Data Storage System (HEC-DSS) model was employed for yearly, seasonal, and monthly analyses of the Euphrates flow rate upon its entry into the Iraqi border at Husaybah city in Anbar Governorate. The standard methodology was employed to assess the duration of particular events by examining their probability of exceeding certain thresholds over time, followed by a cyclical analysis utilizing the P05, P10, P25, P50, and P95 probabilities from the average monthly data. Pearson's correlation coefficient was employed to demonstrate the impact of climate change on the water quantity in the Euphrates River. The Drought Indices Calculator (Drinc) program was utilized to compute the Streamflow Drought Index (SDI) indicators from 1980 to 2022 for three distinct durations: 3 months, 6 months, and 12 months, to analyze drought patterns, severity, and duration at the point where the Euphrates River enters the Iraqi border.

There are insufficient studies evaluating the statistical analyses along the Euphrates River to examine climate change trends; prior research is confined to certain meteorological stations and selected regions along the river. Furthermore, there is an absence of comprehensive statistical analysis about the Euphrates River's flow following its entry into Iraq at Al-Husaybah city, and no evaluation has been performed on its annual, monthly, and seasonal variations influenced by the dams constructed in the upper Euphrates and climatic change. Furthermore, there is no statistical analysis in the previous research illustrating the association between flow rate and climate data. Prior studies concerning the Euphrates River have not assessed drought and its various indicators at the point where water imports from upstream nations enter Iraqi territory.

The article is organized as follows: Section 1 provides an introduction and outlines the study area. Section 2 describes the methodological framework and explains the statistical analysis techniques employed. Section 3 presents the findings and discussions related to the annual trend analysis of precipitation, minimum and maximum temperatures, monthly precipitation, and the trends in maximum and minimum temperatures. This section also covers the variability of annual and monthly precipitation, water flow trend analysis, the correlation between stream flow and climate, and analyses of the hydrological drought index. Finally, Section 4 offers a conclusion summarizing the primary findings.

1.1. Study Area

The Euphrates River is considered a crucial source of surface water in Iraq. The Euphrates River ranks as the fifteenth-longest river in Asia and the longest in Western Asia, measuring 2,780 kilometers. The river is the largest in the Middle East, encompassing a drainage area of 444,000 km², partitioned among Turkey (123,200 km²), Syria (74,800 km²), Jordan (132 km²), Saudi Arabia (66,000 km²), and Iraq (176,000 km²). The river originates in the Taurus Mountains of Turkey, near Keban, where the two tributaries, Furat Su and Murad Su, converge to form the Euphrates River. It flows southwest, crossing into Syria at Jarabulus, receiving three tributaries: Al-Sajur, Al-Balikh, and Al-Khabur. The river then enters Iraq at Husaybah village in Anbar Governorate. It continues southward until it meets the Tigris River at Qurna city, forming the Shatt al-Arab, which empties into the Arabian Gulf. The study is limited to the upper part of the Euphrates River from its entrance at 34°25'21.93"N, 40°59'29.80"E at Husaybah village in Anbar governorate west at the Iraqi border to the Haditha Dam, as shown in Figure 1. Haditha Dam is regarded as a vital dam, notable for its substantial storage capacity of 8.2 billion cubic meters at a height of 147 meters; it is the second-largest dam in Iraq in terms of water storage and hydroelectric power production, following the Mosul Dam. Haditha Dam is an earthen dam situated on the Euphrates River in western Iraq, positioned at latitude 34°12'25.48" N and longitude 42°21'19.14" E, approximately 7 km north of Haditha city and 250 km north of Baghdad governorate. Rainfall and the imports of the Euphrates River from upstream nations are key factors in the Haditha Dam's operation.

Iraq, located in Southwest Asia, exhibits a continental climate marked by significant temperature variations between summer and winter; due to Iraq's geographical position between the arid subtropical Arabian desert and the humid subtropical Arabian Gulf, it results in a hot, dry climate, marked by prolonged, extremely scorching summers and brief, chilly winters. January is the coldest month, with average mean temperatures ranging from 3°C to 12°C, whilst July is often the hottest month, with average mean temperatures reaching 38°C. The annual precipitation in the north is 700 mm, diminishing to 113 mm in the south, while the average temperature has escalated from 35°C in the north to above 45°C in the south. This study utilizes the Husaybah hydrometric station in Iraq as the control gauging station for the upper Euphrates River, using observed surface runoff from this station alongside climate data from the 14 meteorological stations for the period from 1991 to 2022.

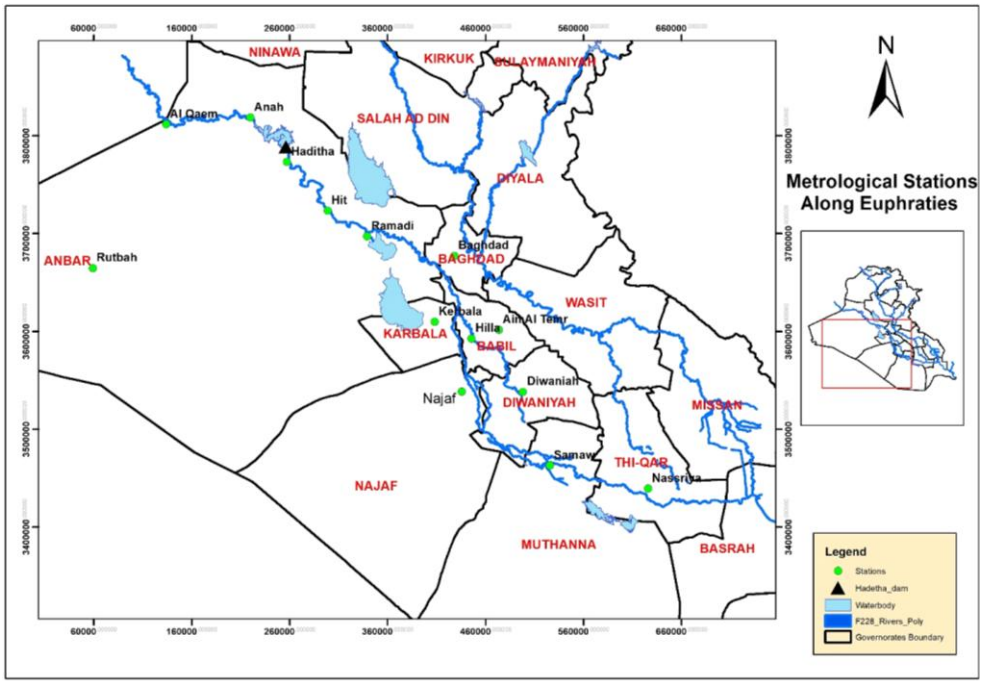

Figure 1. Location of the study area

2. Research Methodology

The Mann–Kendall trend model (MKTM) was used to check for significant changes in yearly rainfall and the maximum and minimum temperatures from 1991 to 2022, using weather data harvested from the Iraqi Ministry of Transportation for 14 meteorological stations: Al-Qaim, Anah, Haditha, Hit, Ramadi, Rutbah, Baghdad, Hilla, Kerbala, Ain Al-Temr, Najaf, Diwaniya, Samawa, and Nassiriya along the Euphrates River. To ensure optimal data utilization, the data gaps found in some meteorological stations were estimated with the inverse distance weighting (IDW) interpolation method. The Sen's slope estimator (SSE) was employed to ascertain the value of this trend. The Mann–Kendall test is a nonparametric test [27-29] applicable when the data do not follow a normal distribution. It is advantageous in situations where data is insufficient in the time series. This test posits the alternative hypothesis.

H1 (indicating an increase or reduction in trend) is accepted, then the null hypothesis H0, which asserts the presence of an effect in data distribution, is rejected. For a specified data set $x1$, $x2$, $x3$, xn, organized in a time series, n denotes the quantity of time series data gathered over the study period. The MK computes the mean statistic S using the following formula:

$$S = \sum_{i=1}^{n-1} \sum_{j=i+1}^{n} sign(xj - xi) \quad (1)$$

where; j = 2, 3…., n; i = 1, 2…., j-1.

$$sign(xj - xi) = -1 \ if \ (xj - xi) < 0$$
$$= 0 \ if \ (xj - xi) = 0$$
$$= 1 \ if \ (xj - xi) > 0$$

A positive number of S signifies an upward trend in the data, whereas a negative value denotes a downward trend. For n≥10, employ the variance computation to approximate the probability outlined by S (Gilbert 1987) [29] using the subsequent formula in case of absence-tied values.

$$VAR(S) = \frac{1}{18}[n(n-1)(2n+5)] \quad (2)$$

The above equation is adjusted to the following formula if there are tied values (difference=0)

$$VAR(S) = \frac{1}{18}[n(n-1)(2n+5) - \sum_{e=1}^{d} te(te-1)(2te+5)] \quad (3)$$

where:

$e = 1, 2 \ldots d$

d = the number of the tied group.

te = the number of data values in the eth group.

A typical standard test statistic, Z, is employed to assess the significance of the trend. If Z is positive, there is an upward tendency; if Z is negative, the trend is downward [30].

Z can be determined using the subsequent equation based on the mean statistic S and the variance of S.

$$Z = \begin{cases} \frac{S-1}{\sqrt{Var(S)}} & for\ S > 0 \\ 0 & for\ S = 0 \\ \frac{S+1}{\sqrt{Var(S)}} & for\ S < 0 \end{cases} \quad (4)$$

The trend of the test is upward. If the value of Z is positive, the opposite is true for negative values, and Z follows a typical normal distribution when Z=0. The significance level of the trend must be evaluated based on the α value to ascertain whether to reject or accept the null hypothesis. This value is determined by the researcher, the sample size, and the significance of the study. This research used a level of 0.05 to assess the trend's significance. When |Z| exceeds Z (c,0.05), the null hypothesis is rejected, indicating a significant trend in the time series. Z (c,0.05) represents the critical value for the normal distribution of the probability Z at (1- α/2), which is 1.96 for a two-tailed test derived from the standard normal distribution table.

Sen's slope estimator (SSE) quantifies the trend slope magnitude in a sample of N data pairs. It is a nonparametric statistical test [31], and the subsequent formula computes a sequence of linear slopes for all data pairs

$$\mu_i = \frac{y_j - y_i}{j-i} \qquad \text{For } 1 \le i < j,\ i < j < N \quad (5)$$

where:

yi, yj are the respective data values at time i and j:

$N = n\,(n-1)/2$

N = no of time series

Then the median of μ_i is equal to Sen's slope estimator = $\mu_{\left[\frac{(N+1)}{2}\right]}$ *If N is odd*

$= \frac{\mu_{[N/2]} + \mu_{[(N+2)/2]}}{2}$ *If N is even*

The sign of the μ_i median indicates whether the trend slope is progressive or regressive, while the median's size assesses the slope's steepness. To compute a confidence interval ($C_\propto$) for the median slope at a designated Z critical for α=0.05 [28, 29], the subsequent formula is employed:

$$C_\propto = Z_{1-\propto/2}\sqrt{Var(S)} \quad (6)$$

where: Var (S) is determined in the Mann-Kendall test: $Z_{1-\propto/2}$ =1.96. Subsequently, compute M1 as $(N - C_\propto)/2$ and M2 as $(N + C_\propto)/2$. The top limit of $C_\propto$ corresponds to the $(M2 + 1)$ th largest value, while the lower limit corresponds to the M1th largest value among the N-ordered slope estimates [29].

HEC-DSS is the U.S. Army Corps of Engineers Hydrologic Engineering Centre Data Storage System. It is designed to store both regular and irregular time series data, and it can retrieve data for any water resources study.

The U.S. Army Corps of Engineers Hydrologic Engineering Centre Data Storage System HEC-DSS can facilitate interaction among several HEC programs. This research analyzed the annual, seasonal, and monthly flow rates of the Euphrates River at Husaybah village by HEC-DSS software to assess the effects of riparian state operational policies and climate change on Haditha Dam inflows and, subsequently, their inverse effects on hydropower generation, public water demand, and agricultural crop water requirements.

Pearson's correlation coefficient is employed to illustrate the linear relationship and its strength between the average monthly discharge of the Euphrates and the average monthly climatic elements, namely rainfall and temperature, as outlined in Equation 7. This analysis aims to evaluate the impact of climate change on the flow rate of the Euphrates.

$$\mathbf{r} = \frac{n\sum x_i y_i - \sum x_i \sum y_i}{\sqrt{n\sum {x_i}^2 - (\sum x_i)^2}\sqrt{n\sum {y_i}^2 - (\sum y_i)^2}} \quad (7)$$

Where; n is the number of data points; x_i, y_i Are the individual sample points indexed with i.

Effective planning and management of water resources necessitate an understanding of hydrological drought. This study utilized the Streamflow Drought Index (SDI), generated from observed monthly runoff data obtained from the Husaybah measuring gauge, to assess hydrological drought. According to Nalbantis & Tsakiris [32]. Suppose a time

series of monthly streamflow volumes Qij is available. In that case, where i represents the hydrological year starting in October and ending in September, j signifies the month within that hydrological year (j = 1 …12), the volume can be derived from Equation 8.

$$V_{i,k} \sum_{j=1}^{3k} Qij \quad (8)$$

Let k = 1, 2, 3, 4, where k = 1 represents 3 months, k = 2 denotes 6 months, k = 3 signifies 9 months, and k = 4 indicates 12 months. $V(i,k)$ represents the cumulative streamflow volume for the i-th hydrological year within the k-th reference period. The Streamflow Drought Index (SDI) is calculated for each reference period k of i hydrological year using Equation 9, based on cumulative streamflow volumes.

$$SDI_{i,k} = \frac{V_{i,k} - \bar{V}_k}{S_k} \quad (9)$$

where $\bar{V}_k$ and S_k denote the mean and standard deviation of the cumulative streamflow volumes during reference period k, as quantified over an extended length, the SDI indicator is categorized under Table 1. Figure 2 presents a diagram of the research framework that was used for this study

Table 1. Classification of hydrological drought based on the SDI index value

SDI Values	
2.0 or more	Extremely Wet
1.5 to 1.99	Severely Wet
1.0 to 1.49	Moderately Wet
0 to 0.99	Mildly Wet
0 to -0.99	Mild Drought
-1.0 to -1.49	Moderately Drought
-1.5 to -1.99	Severe Drought
-2 or less	Extreme Drought

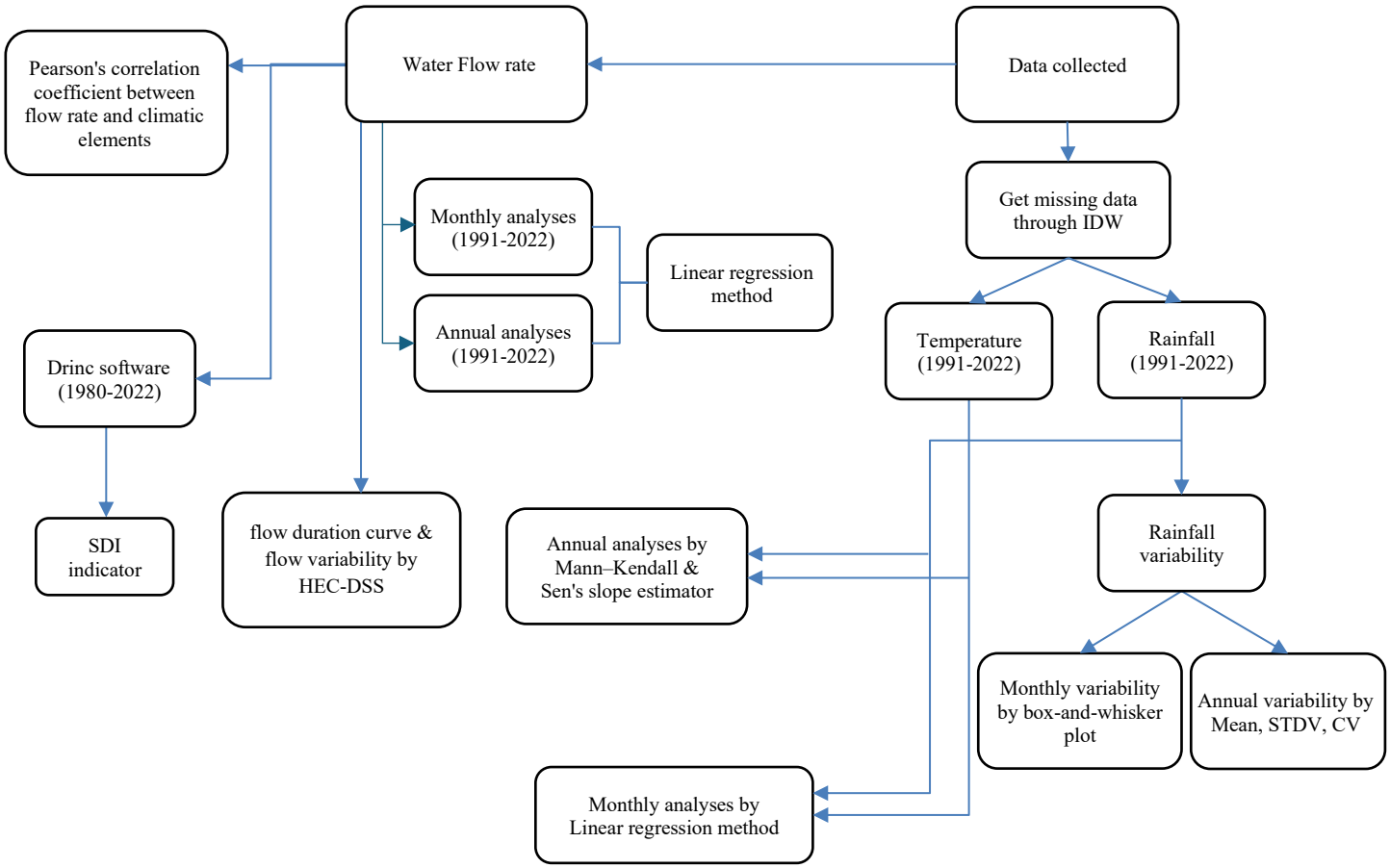

Figure 2. Schematic diagram for the proposed methodology

3. Results and Discussion

3.1. Annual Trend Analysis

The Mann-Kendall test and Sen's slope were employed to assess yearly precipitation and minimum and maximum temperatures at the meteorological stations of Al-Qaim, Anah, Haditha, Hit, Ramadi, Rutbah, Baghdad, Hilla, Kerbala, Ain Al-Temr, Najaf, Diwaniya, Samawa, and Nassiriya along the Euphrates River from 1991 to 2022. The analysis revealed a decline in the yearly rainfall trend of 0.15 mm, as depicted in Figure 3. The maximum annual precipitation was 18.46 mm in 2019, while the minimum was 2.76 mm in 2021. The probability value (P-value) was below the threshold of the trend's significance level. The P-value fell below the significance threshold (α=0.05), signifying the acceptance of the alternative hypothesis (Ha) and the rejection of the null hypothesis (Ho), thereby demonstrating the presence of a significant trend. The Z-statistics of -1.89 confirmed a decline in rainfall trends over the past 32 years, while the standard deviation of 3.99 indicated the dispersion of yearly rainfall from the mean; these facts are presented in Table 2. The Sen's slope test revealed a -0.173 decline in annual rainfall over 32 years, showing an annual deficit rate of -0.173.

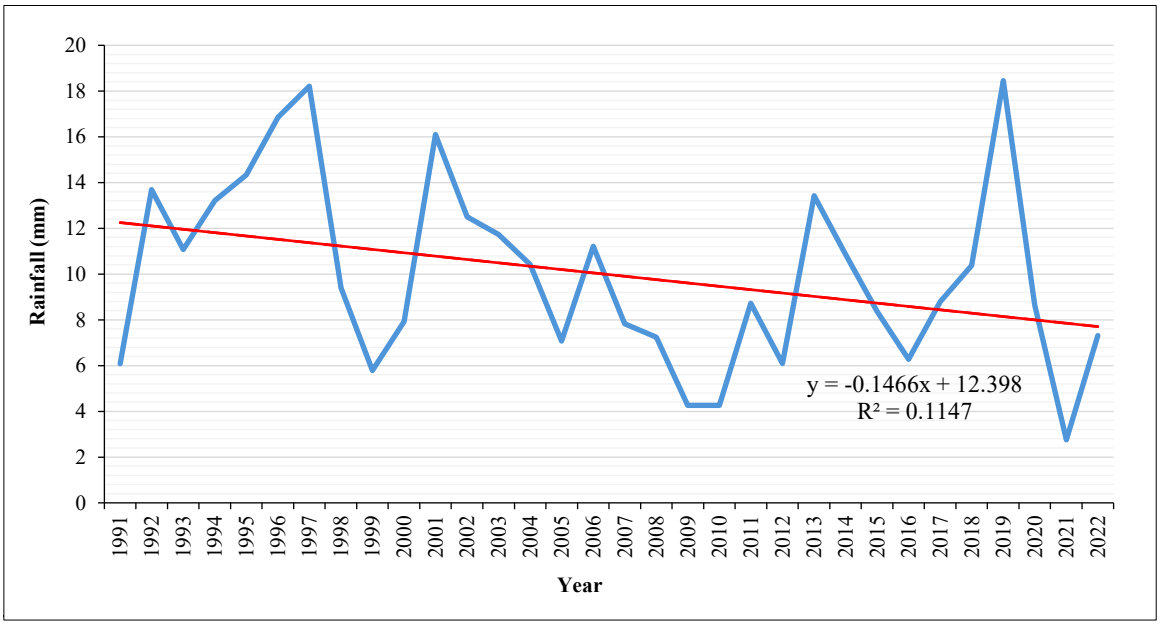

Figure 3. The trend of total yearly precipitation using the Mann-Kendall test from 1991 to 2022

Table 2. Result of the annual rainfall Mann–Kendall trend test

Mann–Kendall trend test result	
Trend	Decreasing
MK-stat	-118
Var (s)	3801.66
P	0.05775
Z-stat	-1.897
STDEV	3.997
Mean	9.98
CV	0.40
Alpha (α)	0.05

Analysis of annual maximum and minimum temperatures, alongside the Sen's slope test over 32 years, indicates a gradual increase in the yearly maximum temperature (Tmax) of 0.086 °C. The peak recorded temperature was 31.63 °C in 2021, while the lowest was 26.06 °C in 1992, as depicted in Figure 3. The trend for minimum temperature (Tmin) indicates an increase of 0.066 °C, with the peak recorded value at 16.32 °C in 2018 and the nadir at 12.54 °C in 1992, as depicted in Figure 4. Table 3 presents the results of this test for yearly maximum and minimum temperatures; the probability value (P-value) was below the significance level (α=0.05) for Tmax and Tmin, suggesting the acceptance of the alternative hypothesis (Ha) and the rejection of the null hypothesis (Ho)> The Zstat values for Tmax and Tmin

corroborate the upward trend observed annually. The standard deviation for maximum temperature (Tmax) is 1.26, suggesting a slight dispersion from the mean, whereas the standard deviation for minimum temperature (Tmin) is 0.92, indicating that the annual data is closely aligned with the mean.

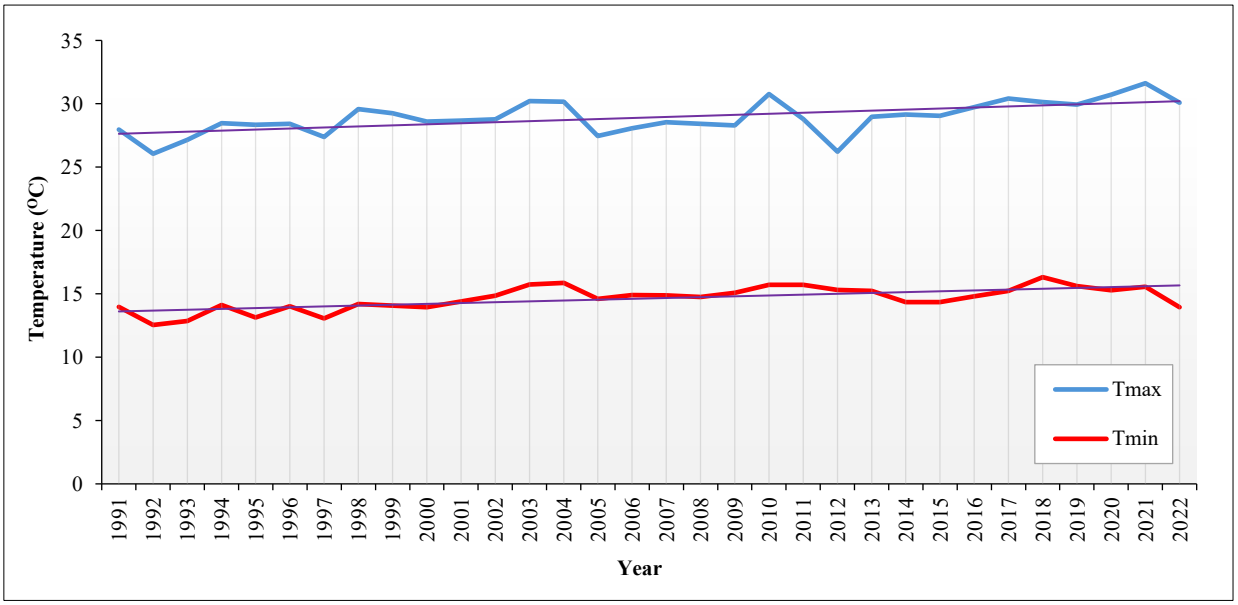

Figure 4. Trend of annual Tmax and Tmin using the Mann-Kendall test from 1991 to 2022

Table 3. Result of the annual temperature Mann–Kendall trend test

Mann–Kendall trend test result	Tmax	Tmin
Trend	increasing	increasing
MK-stat	241	234
Var (s)	3800.66	3798.66
p	9.90233E-05	0.000156
Z-stat	3.89	3.78
STDEV	1.26	0.916
Mean	28.92	14.64
CV	0.043	0.0625
Alpha (α)	0.05	0.05

3.2. Monthly Rainfall, Tmax and Tmin Trend Analysis

The monthly precipitation trend over 32 years is examined by linear regression. Iraq has four distinct seasons: winter from December to March, spring from April to May, summer from June to September, and fall from October to November. Figure 5 illustrates the variation in average monthly precipitation over the four subperiods from 1991 to 2022. Generally, a simple look at the rainfall data (Figure 5) for the four periods (1991-1998), (1999-2006), (2007-2014), and (2015-2022) shows that from January to March (the first three months of the year), the average monthly rainfall was between a high of 32.06 mm and a low of 11.13 mm, with an overall average of 21.60 mm. In April, there was a notable rise of 0.34 mm in the fourth sub-period (2015–2022) due to 2019 being a flood year following the arid years Iraq had from 2008 to 2018, a trend observed since 1933. This month, the average monthly rainfall ranges from 16.69 mm to 8.22 mm, indicating significant climate variations. In May, the average monthly rainfall varies between 9.25 and 3.47 mm, with an average of 6.36 mm; the amount of rain begins to diminish as it marks the conclusion of the spring season. Figure 4 indicates a lack of rainfall from June to September, coinciding with the summer season, which is characterized by elevated temperatures and reduced humidity. During the final quarter of the year (October to December), precipitation begins to rise, commencing in October, the onset of autumn, and culminating in December. Overall, the average monthly rainfall from October to December varies between a minimum of 3.56 mm and a maximum of 29.65 mm, resulting in an average of 16.61 mm.

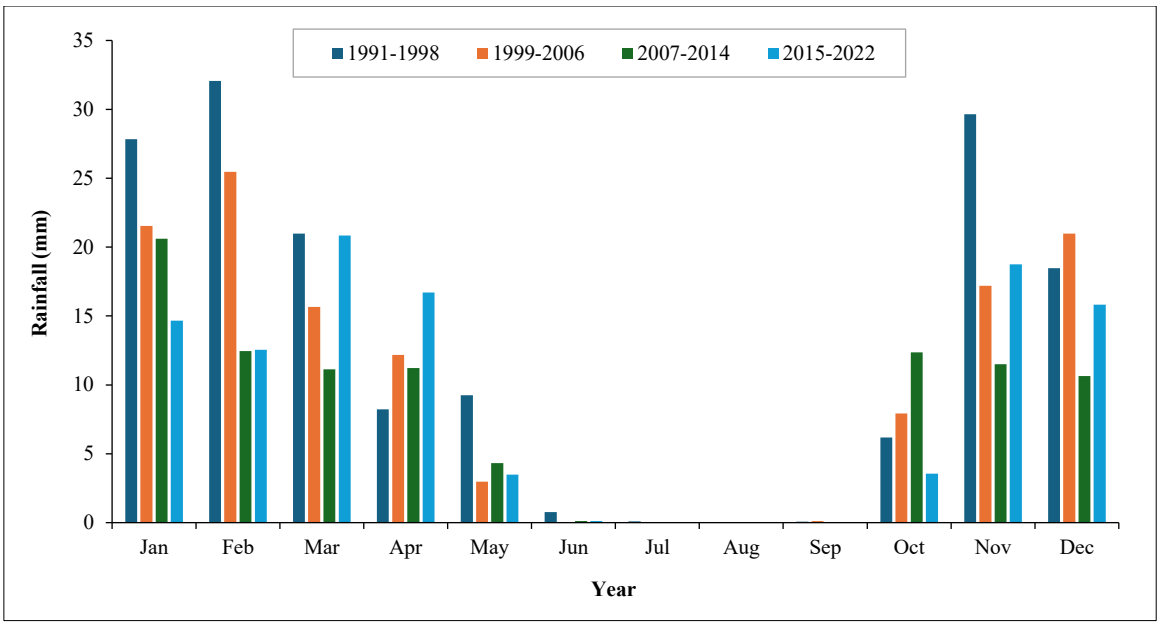

Figure 5. The change in average monthly rainfall for the period 1991–2022

Figure 6 depicts the trend analysis of maximum temperature throughout four intervals: 1991-1998, 1999-2006, 2007-2014, and 2015-2022. In the initial subperiod, the average monthly temperature of January was 13.48°C, temperatures increased in the subsequent months of February, March, April, May, June, and July by 0.13, 0.34, 0.36, 0.20, 0.14, and 0.05, respectively. From August to December, the temperature diminishes by 0.002, 0.09, 0.15, 0.29, and 0.299, respectively. July is the hottest month, reaching 40.6°C, while January is the coldest month, with a temperature of 13.48°C. In January and February of the second, third, and fourth subperiods, the average monthly temperature rose by 0.11, 0.05, 0.17, 0.12, 0.88, and 0.28, respectively, relative to the first subperiod. Conversely, throughout March and April, the second, third, and fourth subperiods experienced a reduction in the average monthly temperature of 0.012, 0.19, 0.28, 0.33, 0.27, and 0.28. In May, the average monthly temperature decreased by 0.24 in the second subperiod and by 0.52 in the third subperiod, while a rise of 0.15 occurred in the fourth subperiod. An elevation in the average monthly temperature was seen in June. In the second and third subperiods, rises of 0.2 and 0.72 were observed, followed by a reduction of 0.19 in the fourth subperiod. From July to December, the temperature rose by 0.59, 0.61, 0.12, 0.045, 0.036, and 0.001, respectively, during the second subperiod. In the third subperiod, the average monthly temperature increased by 0.26 in July, while August experienced a decrease of 0.03. September and October recorded increases of 0.11 and 0.19, respectively, coupled with decreases of 0.10 and 0.06. During the preceding subperiod of July and August, the average monthly temperature increased by 0.37 and 1.46 degrees, respectively. In September, the average monthly temperature decreased by 0.16 degrees; however, in October, it increased by 0.16 degrees. November and December experienced declines in average monthly temperature of 0.11 and 0.02 degrees, respectively.

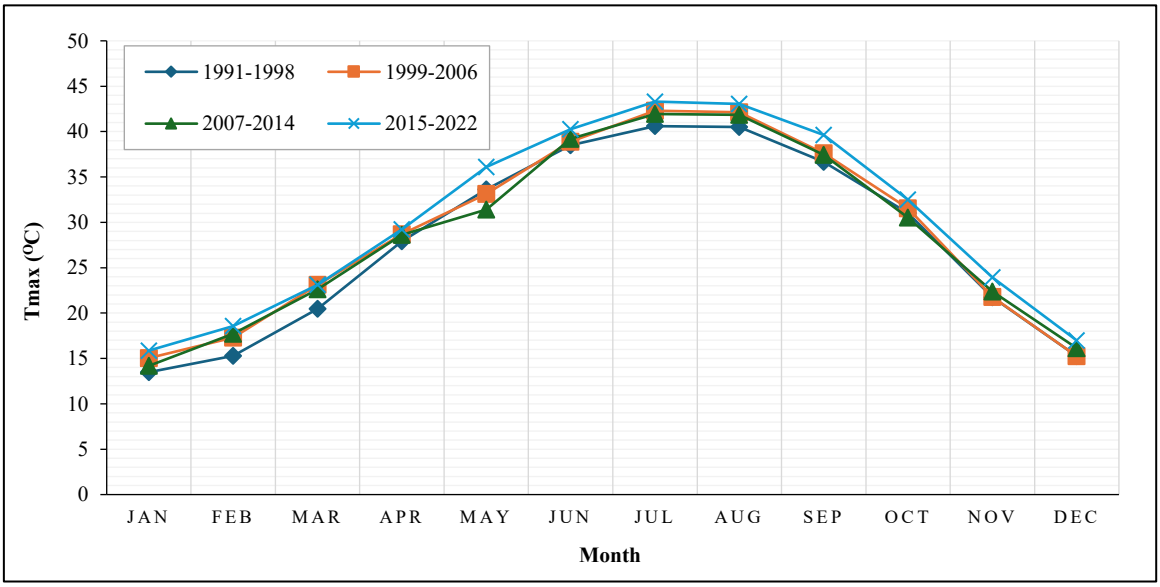

Figure 6. Monthly Tmax trend analysis results from 1991–2022

As illustrated in Figure 7, the analysis of monthly minimum temperature trends reveals that January recorded the lowest average monthly temperature of 2.8°C during the third subperiod (2007-2014). In the subsequent months (February-December), the lowest average monthly temperatures were observed in the first subperiod (1991-1998) as follows: 3.5°C, 7.25°C, 12.45°C, 17.83°C, 22.3°C, 24.55°C, 24.05°C, 19.92°C, 14.72°C, 8.15°C, and 4.03°C, respectively. The highest average monthly temperatures in January and August were recorded in the second subperiod (1999-2006) at 4.25°C and 25.72°C, respectively. The highest average monthly temperatures for February, April, July, and October were noted in the third subperiod, while the remaining months of March, May, June, September, November, and December were recorded in the final subperiod (2015-2022).

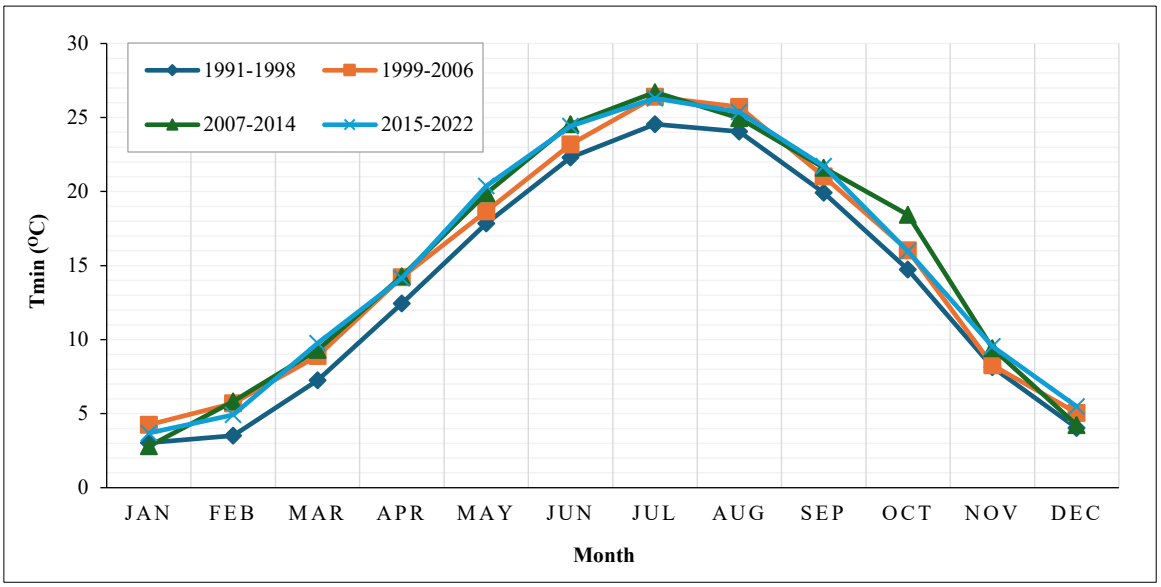

Figure 7. Monthly Tmin trend analysis results from 1991–2022

3.3. Annual Rainfall Variability

Statistical measures were employed to examine the yearly rainfall variations from 1991 to 2022. This analysis covers four specific periods: 1991–1998, 1999–2006, 2007–2014, and 2014–2022. The test results demonstrate that the average rainfall diminishes from the first to the second period, persists in its reduction until the third period, and subsequently undergoes a slight increase in the fourth period. The coefficient variation rose from 28.68% in the initial period to 30.15% in the subsequent period, 37.74% in the third period, and 47.32% in the final period. Water resources management in this region must account for the minor variations in rainfall data, which averaged 2.96 from 2007 to 2014 and subsequently rose to an average of 4.20 from 2014 to 2022, as illustrated in Figure 8 and Table 4. The results indicated the variability of rainfall enhancement during the entire period.

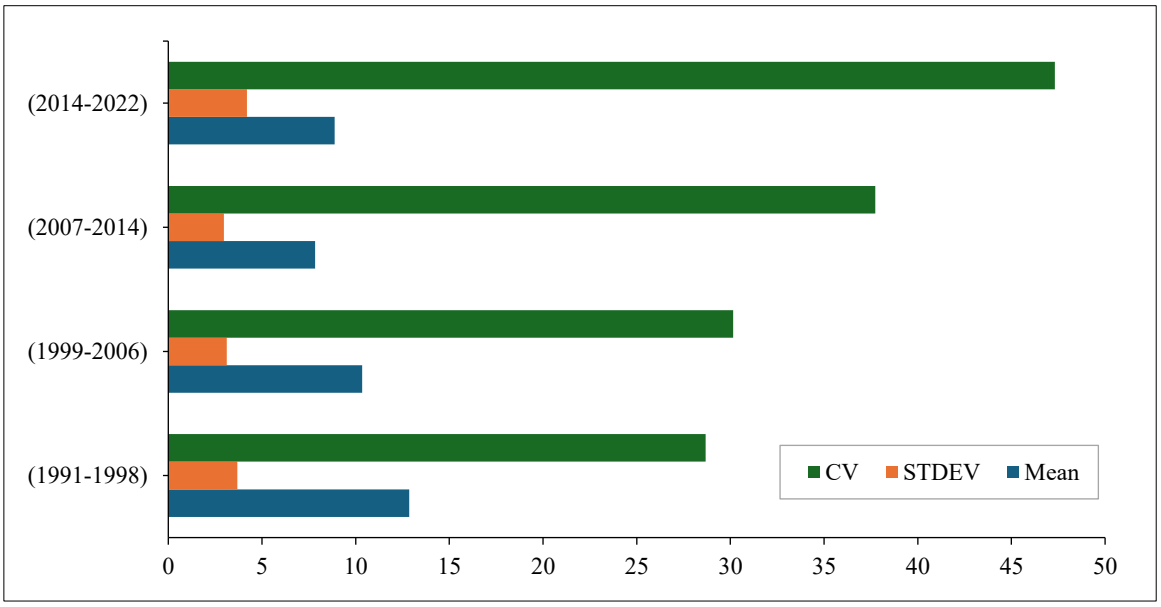

Figure 8. Statistical parameters trend of annual rainfall variability from 1991–2022

Table 4. Variability of annual Rainfall over 32 years from 1991 to 2022

Parameters	(1991-1998)	(1999-2006)	(2007-2014)	(2014-2022)
Mean	**12.86**	**10.34**	**7.84**	**8.87**
STDEV	3.69	**3.12**	**2.96**	**4.20**
CV	**28.68**	**30.15**	**37.74**	**47.32**

3.4. Monthly Rainfall Variability

The box-and-whisker plot depicted the monthly rainfall variations over a span of 32 years, from 1991 to 2022. A box-and-whisker plot can depict the skewness or distribution of the data [33]. The box plot is segmented by the median, indicated by a central line; the upper and lower edges of the box represent the 75th and 25th percentiles, respectively; the extremities of the whiskers denote the 90th, 10th, and 100th percentiles (the maximum values), while the 0th percentile (the minimum values) indicates the lowest amounts. Figure 9 delineates the average monthly rainfall from January to December, recorded as follows: 61.23, 51.93, 32.47, 26.71, 12.02, 0.99, 0.79, 0.07, 0.99, 29.37, 46.61, and 56.34 mm, respectively. This range signifies the difference between each month's maximum and minimum values, suggesting that 50% of the average monthly precipitation lies between these limits. The interquartile range (I.Q.R.) for average monthly rainfall at the 25th and 75th percentiles around the median for January, July, September, and December is 20.89, 0.057, 0.002, and 20.81 mm, respectively. In contrast, the interquartile range (I.Q.R.) for February, March, April, May, June, October, and November is 21.86, 16.83, 11.62, 5.46, 0.057, 9.51, and 20.81 mm, respectively; however, the I.Q.R. for July and August is zero owing to the lack of precipitation during these months. Identified outlier values are 125.25 mm in February; 72.98, 63.62, and 57.85 mm in March; 92.05, 45.79, and 39.56 mm in April; 34.15, 25.95, 20.33, and 15.31 mm in May; 4.07 mm in June; 29.74 mm in October; 95.81 and 87.40 mm in November. Figure 8 shows that the average monthly rainfall for January, March, April, and October is positively skewed, meaning there are more data points above the median than below it. Conversely, February, November, and December display a normal distribution of average monthly rainfall. Statistical characteristics of monthly rainfall variability and analysis are clarified in Table 5.

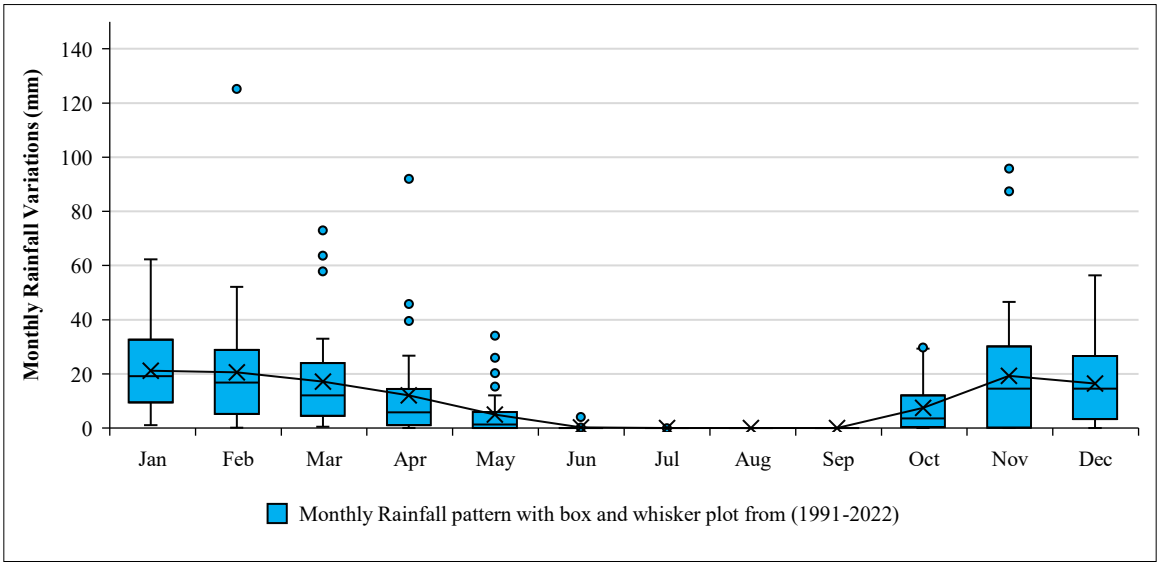

Figure 9. Monthly rainfall pattern with box-and-whisker plot, 1991–2022

Table 5. Statistical characteristics of monthly rainfall variability and analysis table for box-and-whisker plot

Month	Min (mm)	Quartile1 (mm)	Median (mm)	Quartile3 (mm)	Max (mm)	Mean (mm)	SD (mm)	CV%
Jan	1.04	10.06	19.09	30.95	62.28	21.16	15.15	71.58
Feb	0.18	5.19	16.84	27.05	52.12	20.63	23.25	112.7
Mar	0.5	4.66	12.1	21.5	32.98	17.15	17.89	104.34
Apr	0.002	1.2	5.75	12.82	26.72	12.08	18.42	152.47
May	0	0.06	1.25	5.52	12.03	5	8.17	163.36
Jun	0	0	7.63×10^{-6}	0.057	0.99	0.26	0.74	286.99
Jul	0	0	0	0	0.79	0.032	0.14	432.96
Aug	0	0	0	0	0.07	0.006	0.02	309.87
Sep	0	0	0	0.002	1	0.056	0.19	336.75
Oct	0	0.48	3.55	10	29.37	7.5	9.5	127.52
Nov	6.6×10^{-7}	0.17	14.5	29.09	46.62	19.27	22.95	119.05
Dec	0.02	3.75	14.53	24.55	56.37	16.48	14	84.99

3.5. Water Flow Trend Analysis

According to the linear regression analysis, the Euphrates River's annual flow rate at Husaybah village has decreased by 41% over 32 years, as seen in Figure 10. This decrease is explained by Iraq's status as a downstream country, which receives 70% of its water inflows from outside sources but suffers fewer inflows from its neighbors as a result of upstream countries' foreign policies. Iraq was considered a water-rich country until the early 1970s, but when Turkey started the GAP project, signs of a water shortage disaster appeared. This project, which began in the 1970s, included numerous irrigation, agricultural, and industrial projects in addition to the building of 14 dams on the Euphrates River and 19 hydroelectric power plants for the newly formed provinces in southeast Turkey. Furthermore, the region's water, food, energy, and environmental security have all suffered as a result of climate change, which has exacerbated global warming and prolonged droughts. The lowest flow rate, 221 m³/s, was recorded in 2022, while the highest annual average flow rate, 9.947 m³/s, was recorded in 1996. Figure 11 displays the monthly average flow rate evaluations from 1991 to 2022, along with the maximum, minimum, and average values. A thorough grasp of the annual streamflow pattern can be achieved by performing a monthly analysis, between January and December, the maximum average monthly flow rate trend decreased by 32%, and the trend of minimum average monthly flow rate increased slightly by 2.1%, but the mean average monthly flow rate decreased by 11.6%.

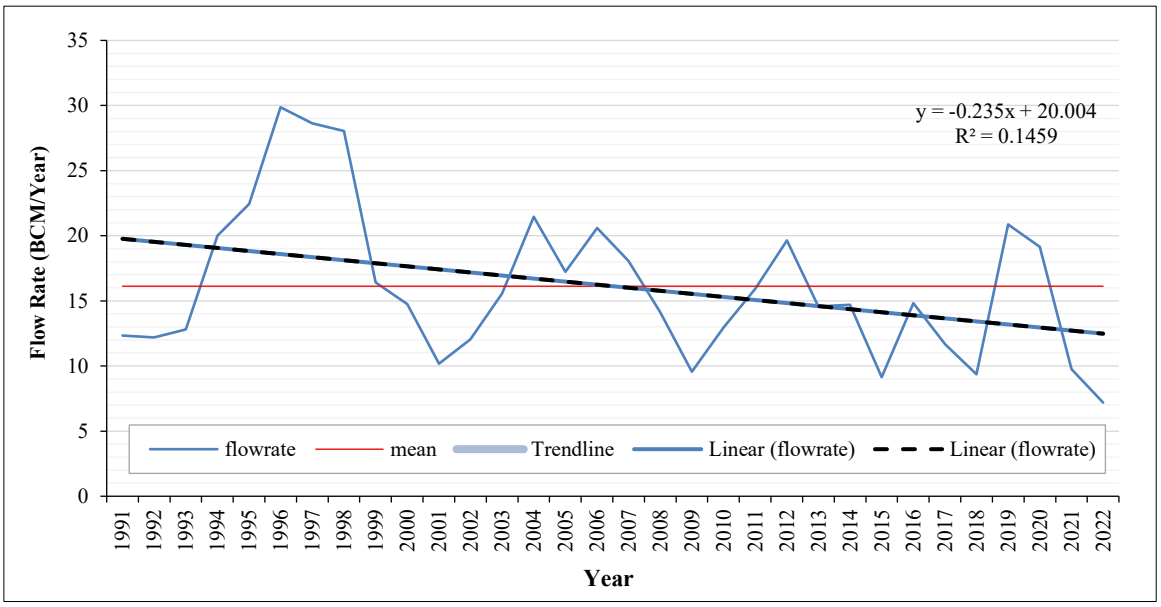

Figure 10. Yearly Euphrates flow rate, 1991–2022

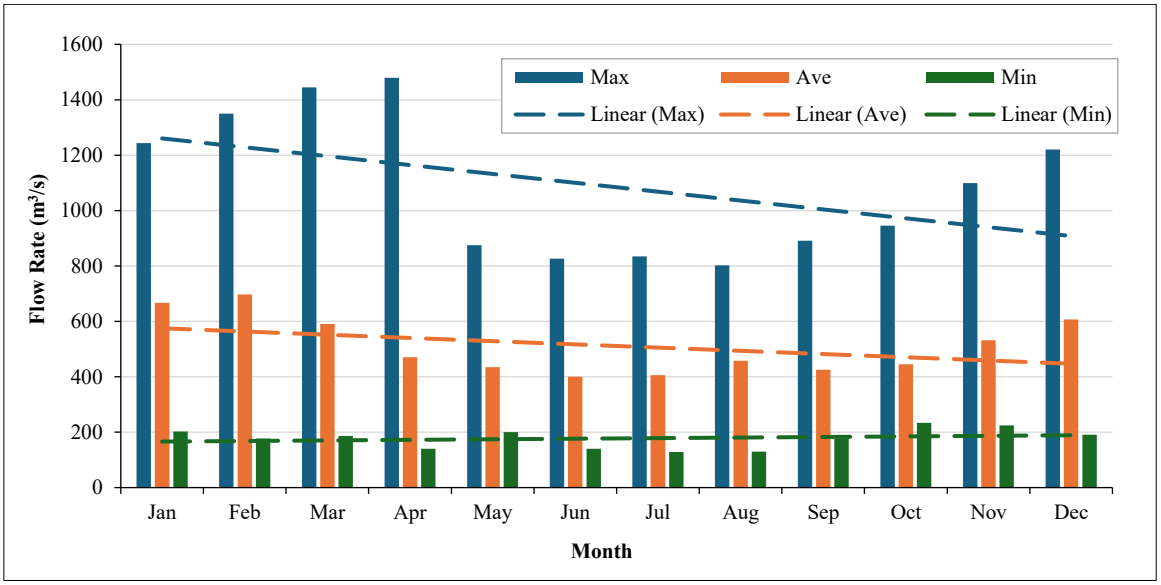

Figure 11. Monthly analysis of the Euphrates flow rate, 1991–2022

The U.S. Army Corps of Engineers Hydrologic Engineering Centre Data Storage System (HEC-DSS) software was utilized to analyze the flow duration curve and evaluate the flow variability of the Euphrates River over 32 years within

Iraqi territory. This method illustrates that the flow probability will meet or exceed the time percentage (Subramanya, 2023), which is essential for hydropower design and water resource management planning. The data on the annual flow duration curve reveal that Q10 at a 10% probability is 850 m³/s, Q40 at a 40% probability is 526 m³/s, Q50 at a 50% probability is 446 m³/s, and Q90 at a 90% probability is 251 m³/s, as depicted in Figure 12.

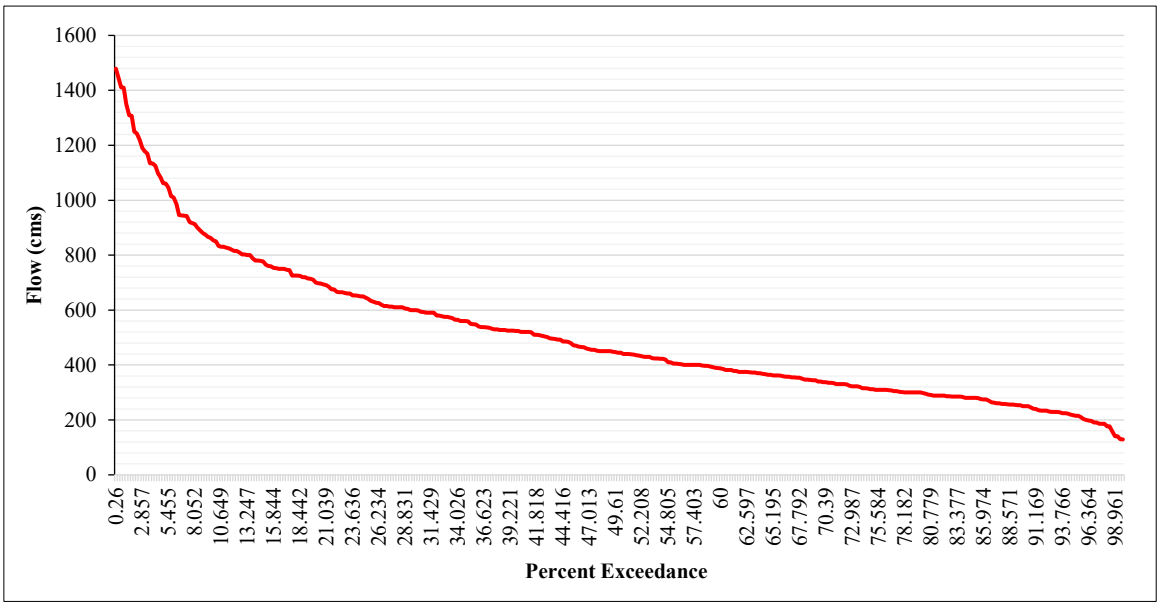

Figure 12. Duration curve of annual Euphrates flow rate at Husaybah city, 1991-2022

For seasonal flow duration curve (FDC) analysis, the study period was split into four seasons: January through March, April through June, July through September, and October through December. At a 1% probability, the highest first quartile Q1 in the second seasonal period is 1480 m³/s, while the minimum for the third seasonal period is 893 m³/s, as shown in Figure 13. The highest flow during the Jan–Mar seasonal period exceeded 50% of the time, at 601 m³/s, and the minimum flow during the April–June period exceeded 373 m³/s for the median flow second quartile Q50. Finally, the maximum flow of 288 m³/s exceeded 90% of the time in the first period, while the minimum was 220 m³/s in the second seasonal period.

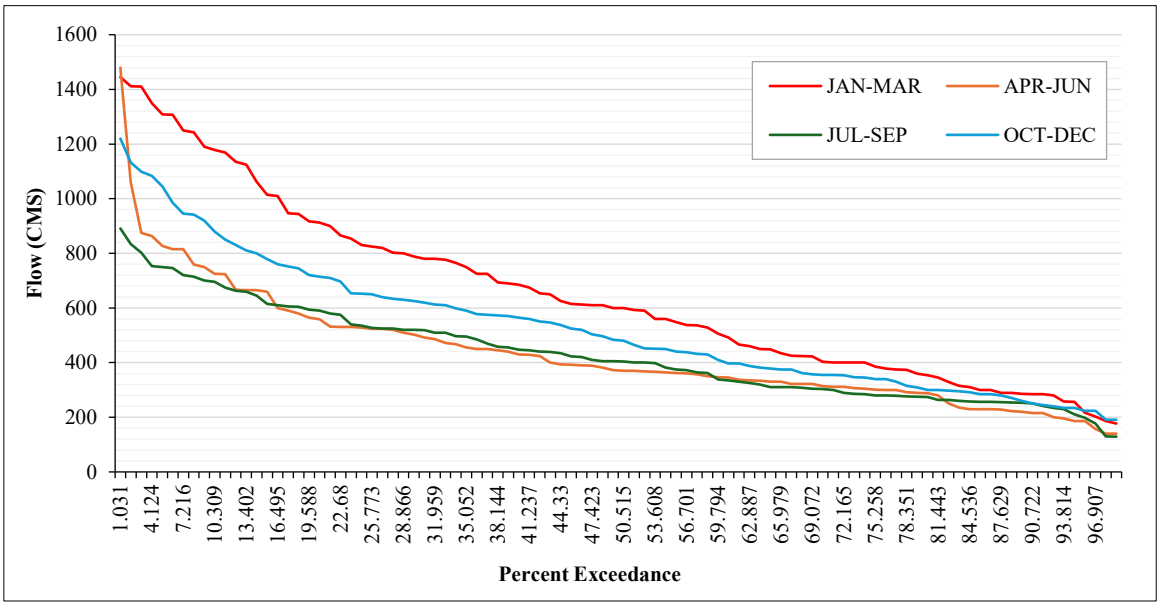

Figure 13. Duration curve of seasonal Euphrates flow rate at Husaybah city, 1991-2022

According to Figure 14, the monthly flow duration curve FDC analyses show that the maximum 10th quartile Q10 at 10% probability is 1411 m3/s in March, the minimum is 667m3/s in June, the maximum 40th quartile Q40 at 40% probability is 765 m3/s in January, the minimum is 406 m3/s in June and July, the maximum second quartile Q50 at 50% probability is 653 m3/s in February, the minimum is 369 m3/s in May, June, July, and October, and the maximum 90th quartile Q90 at 90% probability is 301 m3/s in February, the minimum is 187 m3/s in April and June.

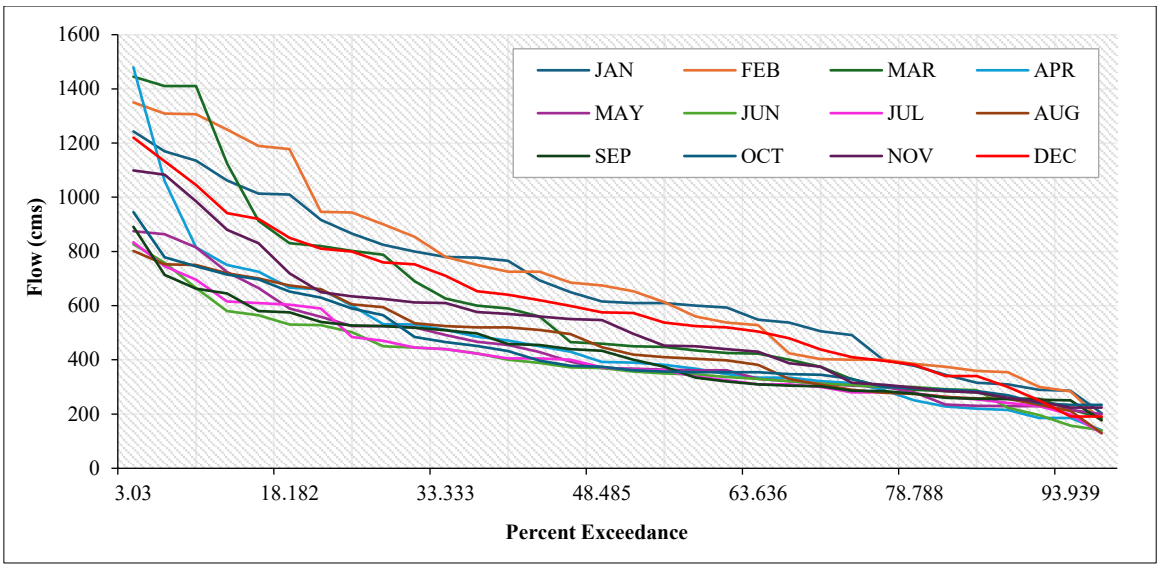

Figure 14. Duration curve of monthly Euphrates flow rate at Husaybah city, 1991-2022

Percentile statistical analyses were conducted for the monthly Euphrates flow rate (1991–2022) to produce a discharge distribution at or below a specific percentile (P05, P10, P25, P50, P75, P90, and P95) with the maximum and minimum values provided. The highest notable monthly flow rate (maximum) from January through April is 1480 m3/s. According to Figure 15, it fell sharply to 875 m3/s in May, remained there through June and July, then decreased slightly in August before rising again in September. The following months saw a minor increase, reaching 1220 m3/s in December. The minimum flow is lowest in July (129 m3/s) and August (130 m3/s). The 50th percentile represents the median value of a given data set; the 90th and 95th percentiles are noteworthy for low flow indicators, and the 05th percentile denotes a substantial amount of high flow.

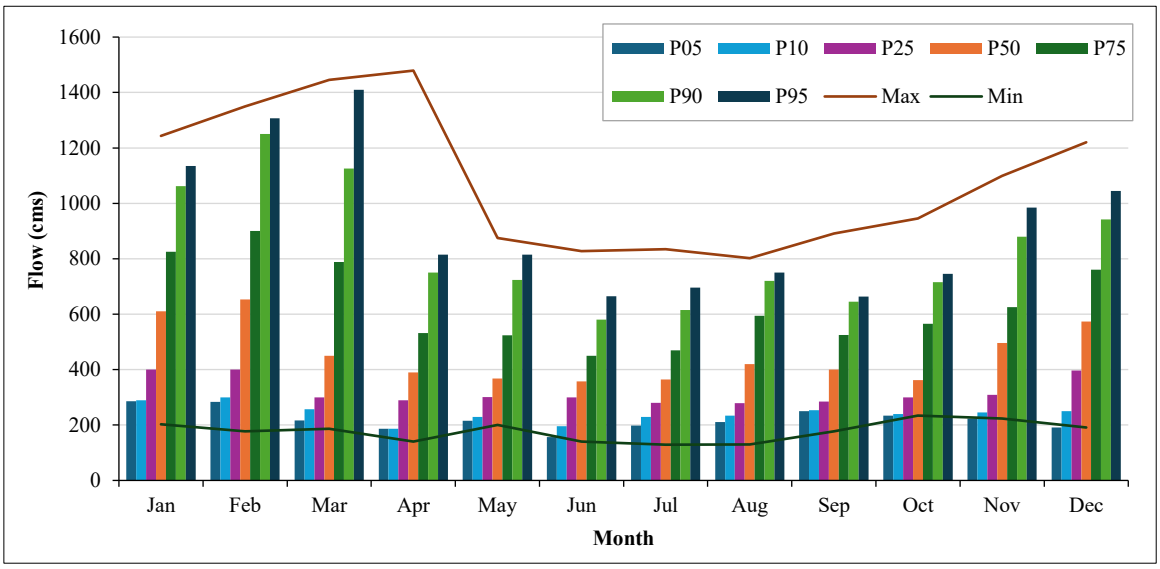

Figure 15. Cyclic Analysis of monthly Euphrates flow rate (1991–2022)

The monthly flow rate of the Euphrates River demonstrates a cyclical pattern, predominantly affected by seasonal precipitation and water management strategies. Peak flow rates often occur during the spring months, March to May, as a result of snowmelt and precipitation in the upstream regions, especially in Turkey. Flow rates diminish in the summer and autumn months due to heightened upstream water storage and evaporation. The construction of dams and barrages, particularly in Turkey, has markedly modified the natural flow regime, resulting in diminished downstream flow, especially during periods of low flow. The maximum values for the 5th and 25th percentiles recorded in January are 286 m^3/s. In February, the maximum values for the 10th, 25th, 50th, 90th, and 95th percentiles are 300 m^3/s, 400 m^3/s, 900 m^3/s, and 1410 m^3/s, respectively, as February is characterized by the highest rainfall. In June, the minimum values recorded were 157 m^3/s for the 5th percentile, 286 m^3/s for the 50th percentile, 450 m^3/s for the 75th percentile, and 580 m^3/s for the 90th percentile, respectively. The minimum value for the 10th percentile was identified in April at 286 m^3/s, while the minimum value for the 25th percentile was noted in August at 279 m^3/s. The minimum value of the 95th percentile, recorded in September, is 663 m^3/s.

3.6. Relationship of Stream Flow and Climate

The correlation coefficient is a statistical measure that is employed to illustrate the intensity and direction of the linear relationship between the average monthly flow rate of the Euphrates River and both maximum and minimum temperatures, as well as between the monthly flow rate of the Euphrates River and precipitation. Based on Table 6, Figures 16 and 17, it is evident that there is a negative low correlation of 0.36 between the average monthly flow rate and the average monthly minimum and maximum temperatures. Conversely, there is a positive low correlation of 0.29 between the monthly flow rate of the Euphrates River and precipitation, as clarified in Figure 18.

Table 6. Range of Correlation Coefficient Values and the Corresponding Levels of Correlation

Scale of the correlation coefficient	Value
$0 < r \leq 0.19$	Very low correlation
$0.2 \leq r \leq 0.39$	low correlation
$0.4 \leq r \leq 0.59$	Moderate correlation
$0.6 \leq r \leq 0.79$	High correlation
$0.8 \leq r \leq 1$	Very High correlation

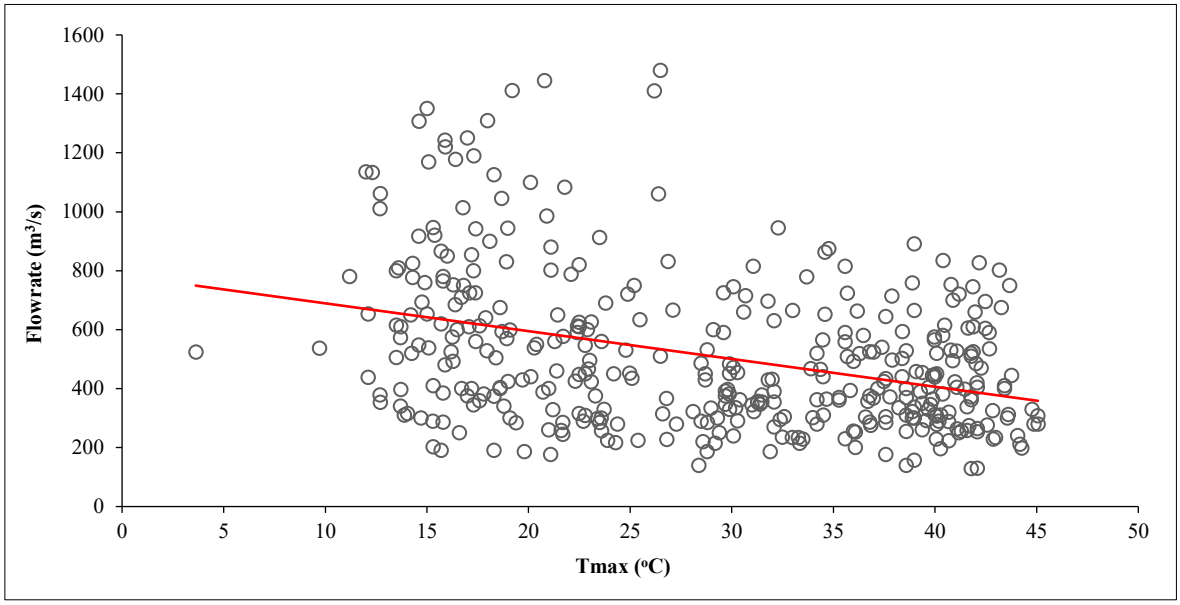

Figure 16. Linear relationship between flow rate and maximum temperature

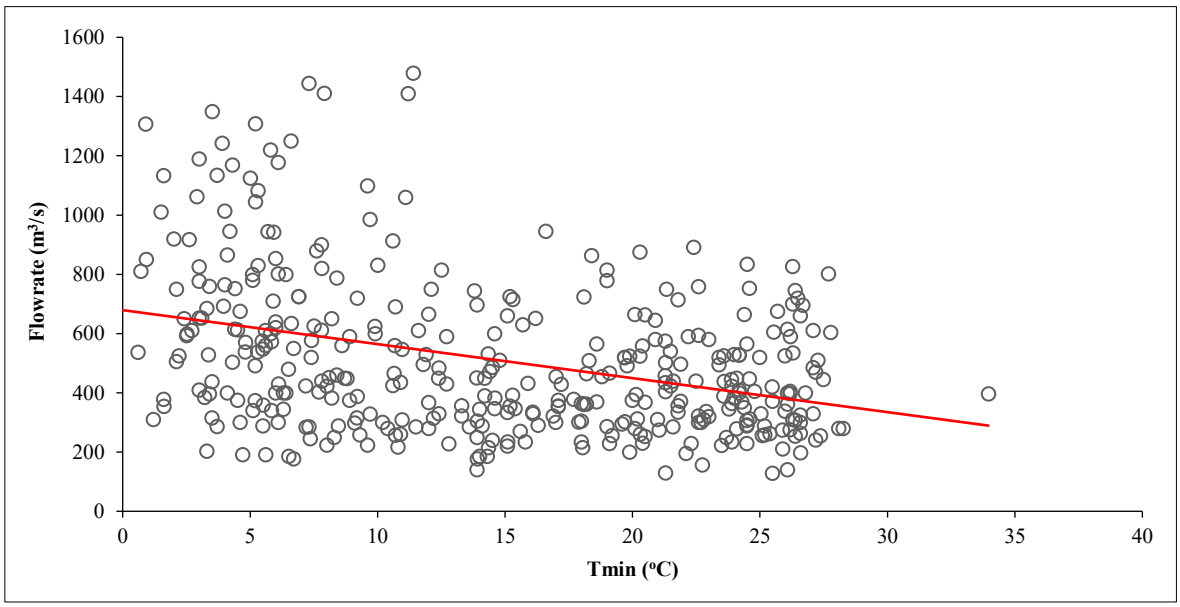

Figure 17. Linear relationship between flow rate and minimum temperature

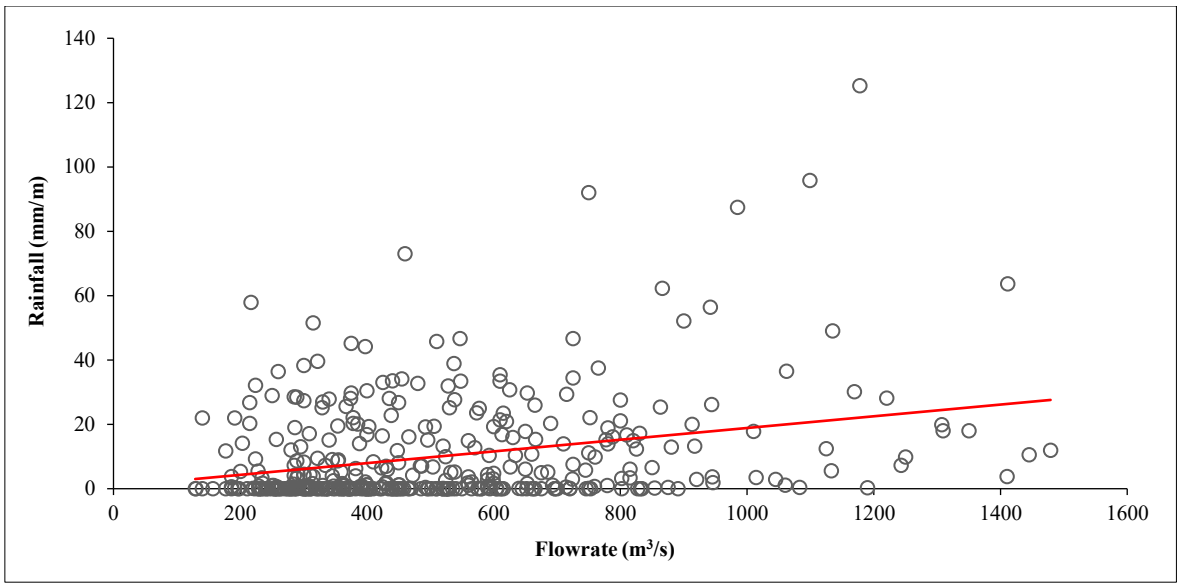

Figure 18. Linear relationship between flow rate and rainfall

3.7. Hydrological Drought

The Drought Indices Calculator Drinc software was utilized to compute the SDI indicators from 1980 to 2022 for three-month, six-month, and twelve-month periods. The analysis results shown in Table 1 indicate that during the water year 1987-1988, the three-month period revealed a significant wet condition, with an SDI of 4.05 (April-June), as shown in Figure 19. There was only one instance of extremely wet conditions, which had a total chance of 2.38% across all three-month periods studied, except for July-September, where it occurred twice with a chance of 4.76%, as shown in Table 7 and Figures 20 and 21 for frequency and probability analysis. Mild drought conditions were recorded in the years 1985-1986, 1990-1991, 1991-1992 (October-December), 1992-1993, 2001-2002, 2002-2003, 2007-2008, 2008-2009 (July-September), 2009-2010, 2012-2013, 2013-2014, 2016-2017 (April-June), 2017-2018 (April-June), and 2020-2021, exhibiting a frequency of 8 and a probability of 19.05% for the periods of October-December and April-June, alongside a frequency of 5 and a probability of 11.90% for January-March and July-September. The following years registered moderate drought conditions: 1988-1989, 1989-1990 (October-December), 1991-1992 (July-September), 1998-1999, 1999-2000, 2000-2001, 2008-2009 (October-December), 2009-2010 (January-March), 2014-2015 (October-December), 2016-2017 (July-September), 2017-2018 (July-September), 2018-2019 (January-March), and 2021-2022 (July-September), with a frequency of 5 and a probability of 11.90% for the periods of October-December and April-June, a frequency of 6 and a probability of 14.29% for January-March, and a frequency of 7 and a probability of 16.67% for July-September. The years 1989-1990 (January-March), 2018-2019 (October-December), 2020-2021, and 2021-2022 (October-December) recorded severe drought conditions. A notable drought occurred from July to September in the water year 2014-2015 and from January to March in 2021-2022, with a frequency of 1 and a probability of 2.38%.

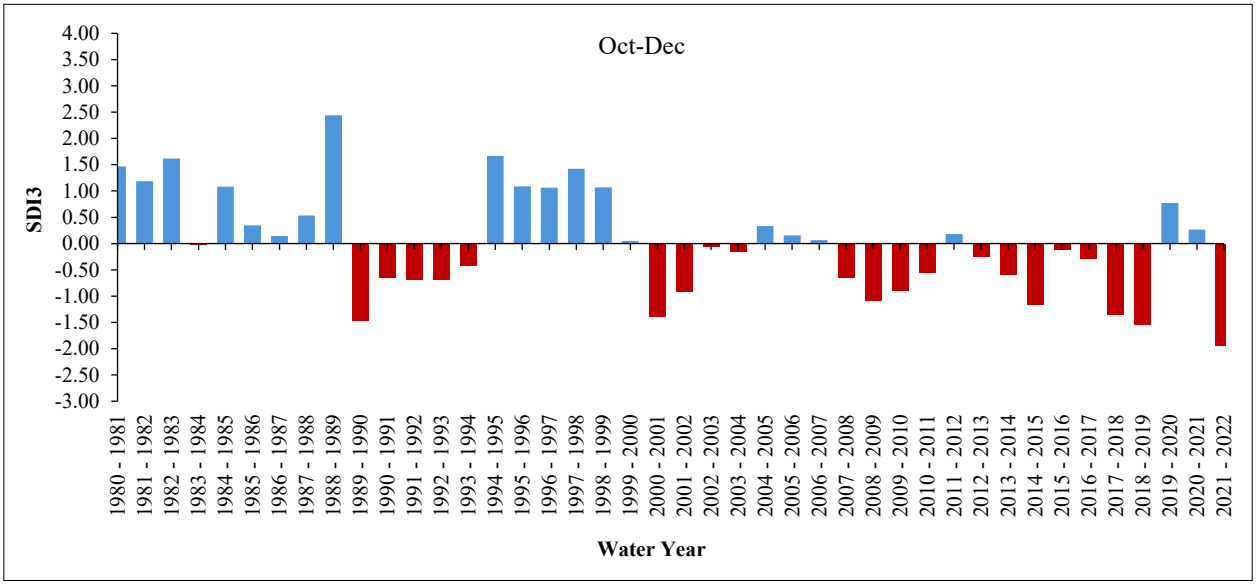

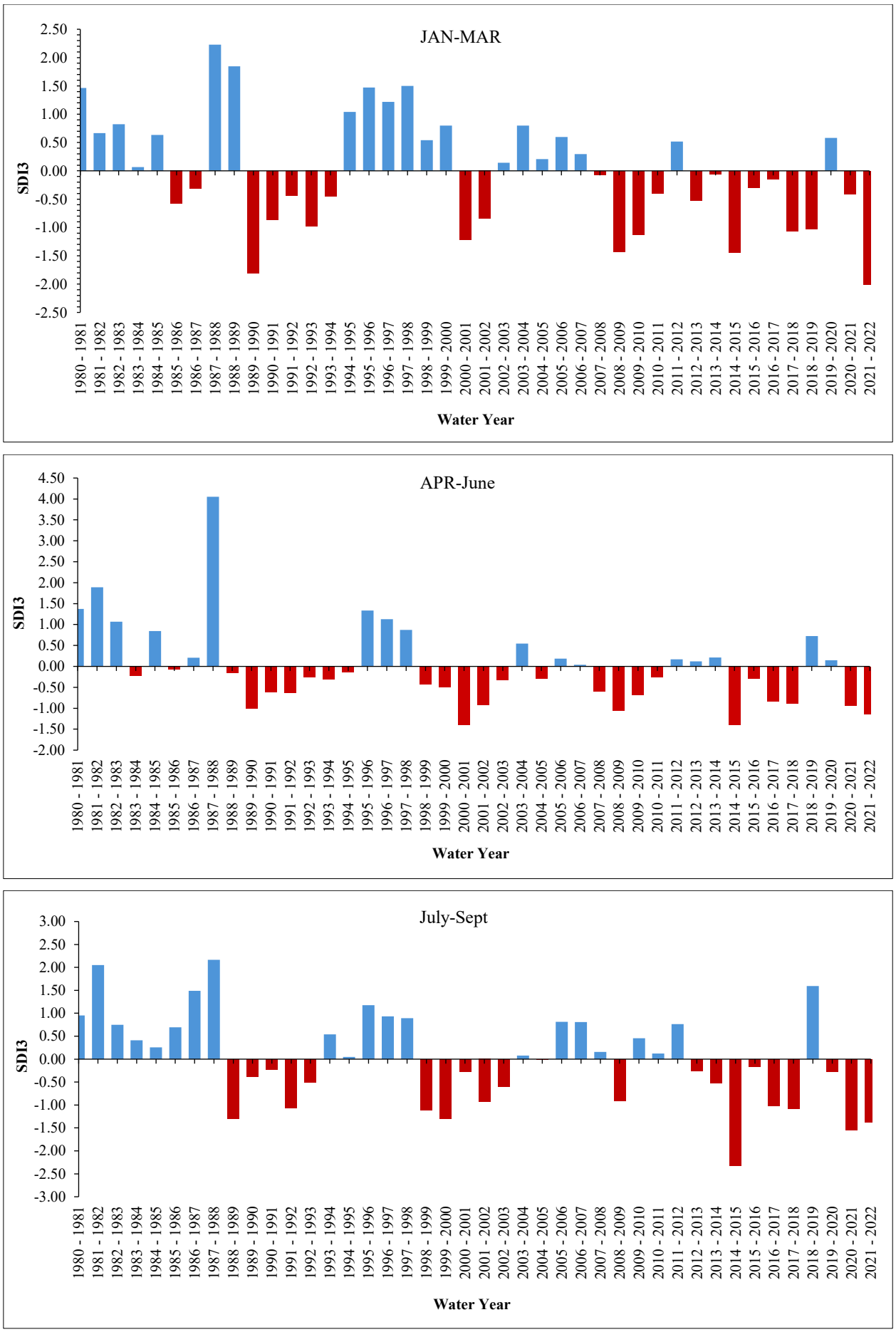

Figure 19. Temporal variation in seasonal SDI3 according to the flow observation station Husaybah in the Euphrates basin

Table 7. Frequency and probability percentage of seasonal SDI3 drought from 1980-2022

Severity	Frequency				Percentage			
	Oct-Dec	Jan-Mar	April-June	July-Sept	Oct-Dec	Jan-Mar	April-June	July-Sept
Extremely wet	1	1	1	2	2.38	2.38	2.38	4.76
Severely wet	2	1	1	1	4.76	2.38	2.38	2.38
Moderately wet	7	5	4	2	16.67	11.90	9.52	4.76
Slightly wet	2	9	4	9	4.76	21.43	9.52	21.43
Normal	15	13	19	14	35.71	30.95	45.24	33.33
Mild drought	8	5	8	5	19.05	11.90	19.05	11.90
Moderately drought	5	6	5	7	11.90	14.29	11.90	16.67
Severely drought	2	1	0	1	4.76	2.38	0	2.38
Extremely drought	0	1	0	1	0	2.38	0	2.38

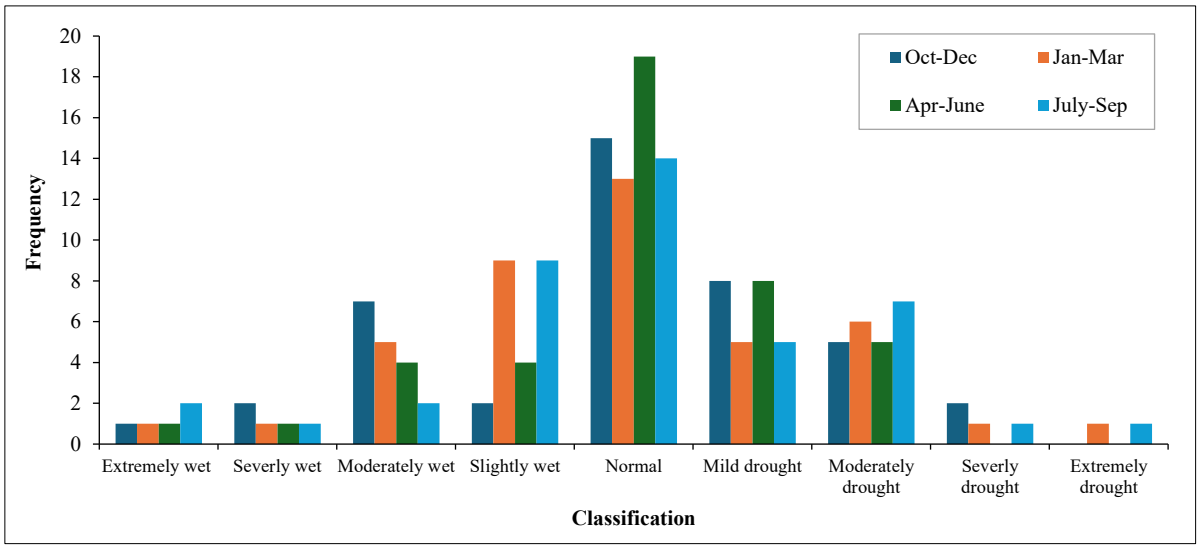

Figure 20. Seasonal SDI3 drought successive reoccurrence interval from 1980-2022

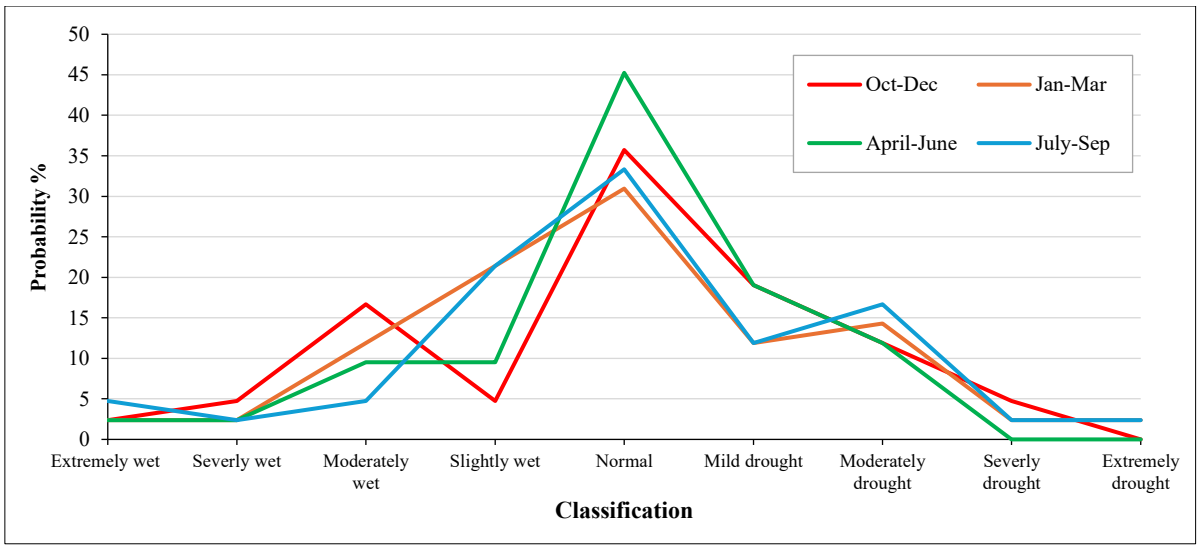

Figure 21. Probability of Seasonal SDI3 drought from 1980-2022

The water year 1987–1988 appeared to be an exceptionally wet year with an SDI of 3.60 from April to September for the six-month SDI6 drought indicator, as seen in Figure 22. Table 8, Figures 23, and 24 for frequency and probability analysis show that severe wet conditions were documented once from October to March (probability 2.38%) and twice from April to September (probability 4.76%). The years 1988-1989, 1989-1990, 1990-1991, 1991-1992, 1992-1993, 1998-1999, 1999-2000, 2000-2001 (April–September), 2001-2002, and 2016-2017 all had mild drought conditions.

These years showed a frequency of 4 with a probability of 9.52% for the October–March period and 8 with a probability of 19.05% for the April–September period. The following years had moderate drought conditions: 2000-2001 (October-March), 2008-2009, 2009-2010, 2014-2015, 2017-2018, 2018-2019, 2020-2021, and 2021-2022. The October to March interval had a frequency of 6 and a probability of 14.29%, while the April to September interval had a frequency of 4 and a probability of 9.52%. In the years 1989–1990 and 2014–2015, there were severe drought conditions; in 2021–2022, there was an intense drought event from October to March, with a frequency of 1 and a probability of 2.38%.

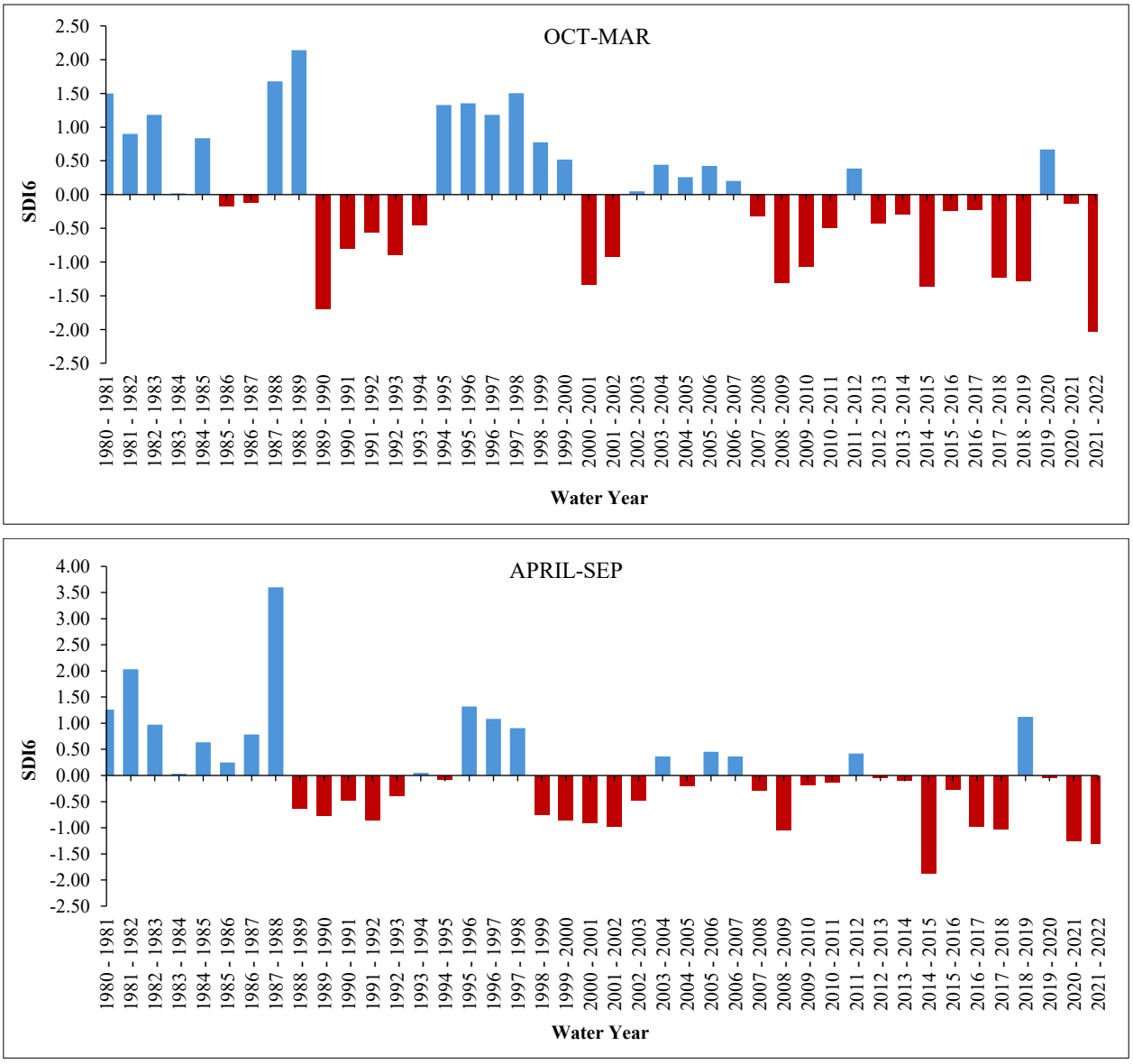

Figure 22. Temporal variation in SDI6 according to the flow observation station Husaybah in the Euphrates basin

Table 8. Frequency and probability percentage of Semi-annual SDI6 drought from 1980-2022

Severity	Frequency		Percentage	
	Oct-March	April-Sept	Oct-March	April-Sept
Extremely wet	1	2	2.38	4.76
Severely wet	2	0	4.76	0
Moderately wet	5	4	11.90	9.52
Slightly wet	5	4	11.90	9.52
Normal	17	19	40.48	45.24
Mild drought	4	8	9.52	19.05
Moderately drought	6	4	14.29	9.52
Severely drought	1	1	2.38	2.38
Extremely drought	1	1	2.38	0

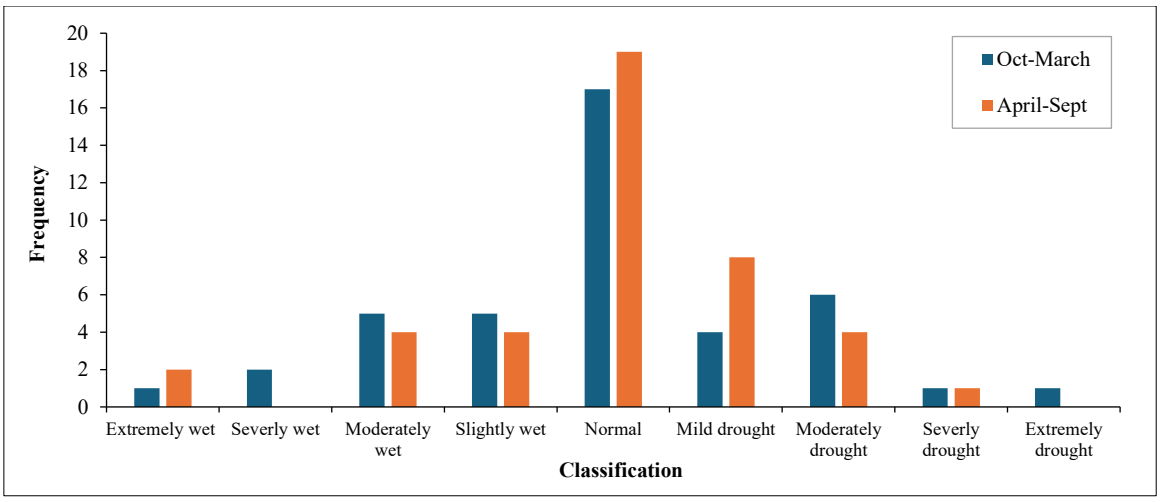

Figure 23. Semi-annual SDI6 drought successive reoccurrence interval from 1980-2022

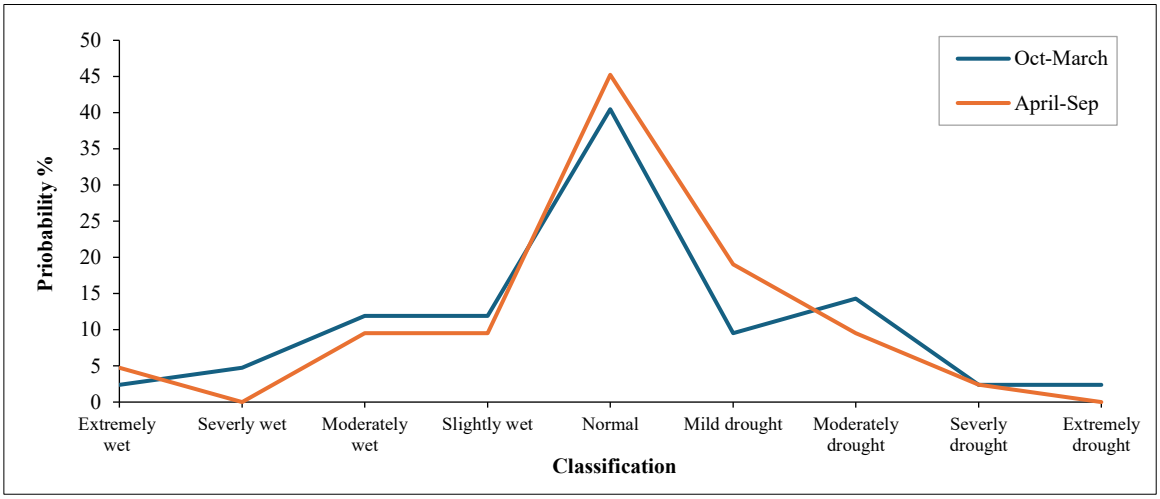

Figure 24. Probability of Semi-annual SDI6 drought from 1980-2022

The analysis of the annual drought period indicated that the water year 1987-1988 saw an exceptional wet condition, demonstrated by an SDI12 of 2.84 from October to September, as shown in Figure 25. Extremely wet conditions were documented once, with a probability of 2.38%, as illustrated in Table 9 and Figures 26 and 27 for frequency and probability analysis. Mild drought conditions were documented in the years 1990-1991, 1991-1992, 1992-1993, 2009-2010, 2016-2017, and 2020-2021, happening six times with a chance of 14.29%. Moderate drought conditions were observed in 1989-1990, 2000-2001, 2001-2002, 2008-2009, and 2017-2018, occurring with a frequency of 5 and a probability of 11.90%. Severe drought conditions have been observed for the periods of 2014-2015 and 2021-2022, occurring twice, with a chance of 4.76%.

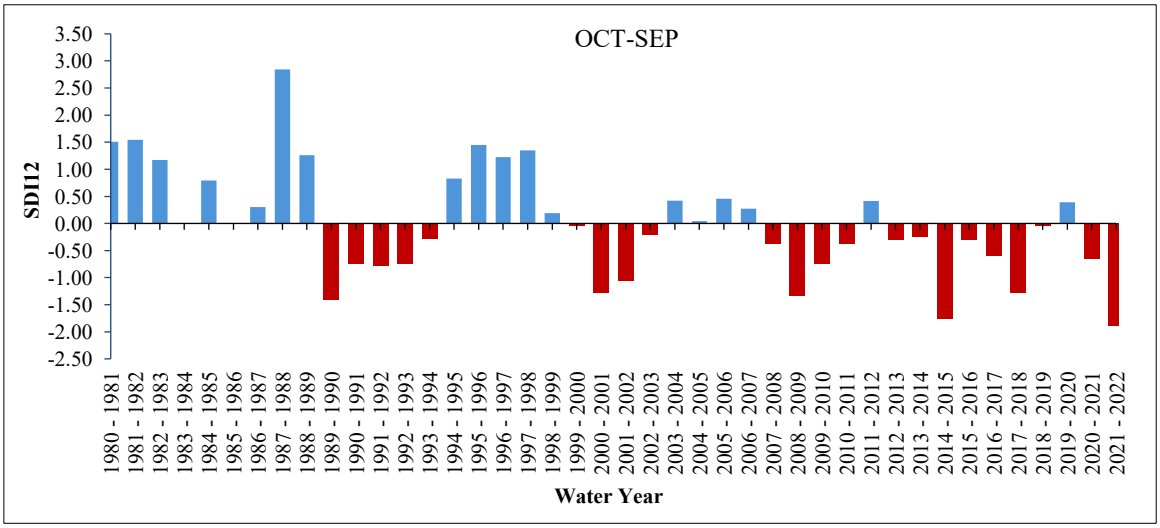

Figure 25. Temporal variation in annual SDI12 according to the flow observation station Husaybah in the Euphrates basin

Table 9. Frequency and probability percentage of annual SDI12 drought from 1980-2022

Severity	Frequency	Percentage
	Oct-Sept	Oct-Sept
Extremely wet	1	2.38
Severely wet	2	4.76
Moderately wet	5	11.90
Slightly wet	2	4.76
Normal	19	45.24
Mild drought	6	14.29
Moderately drought	5	11.90
Severely drought	2	4.76
Extremely drought	0	0

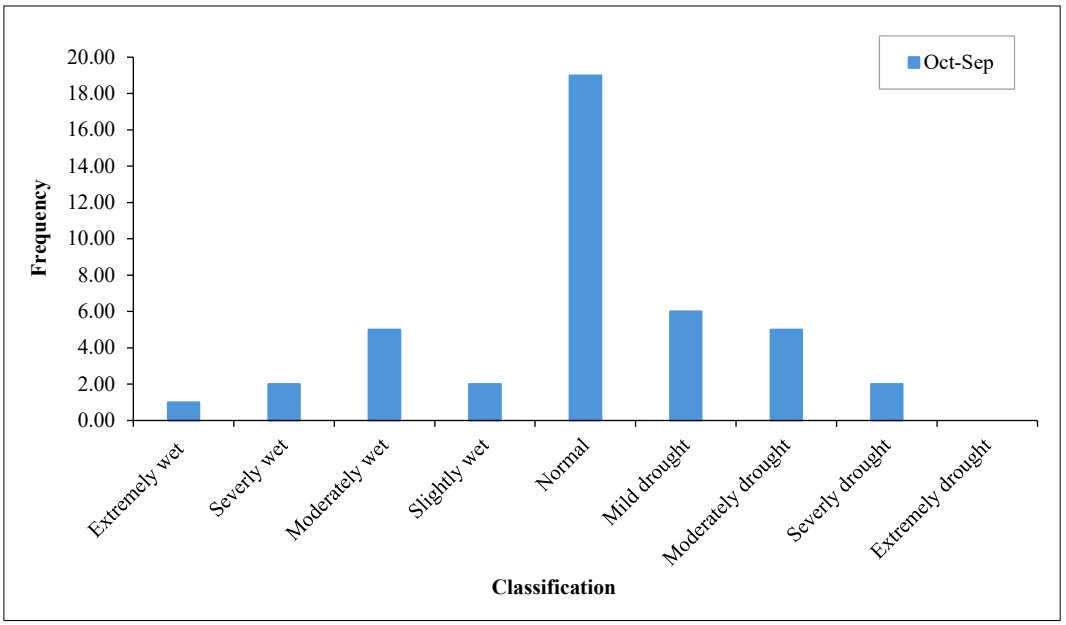

Figure 26. Annual SDI12 drought successive reoccurrence interval from 1980-2022

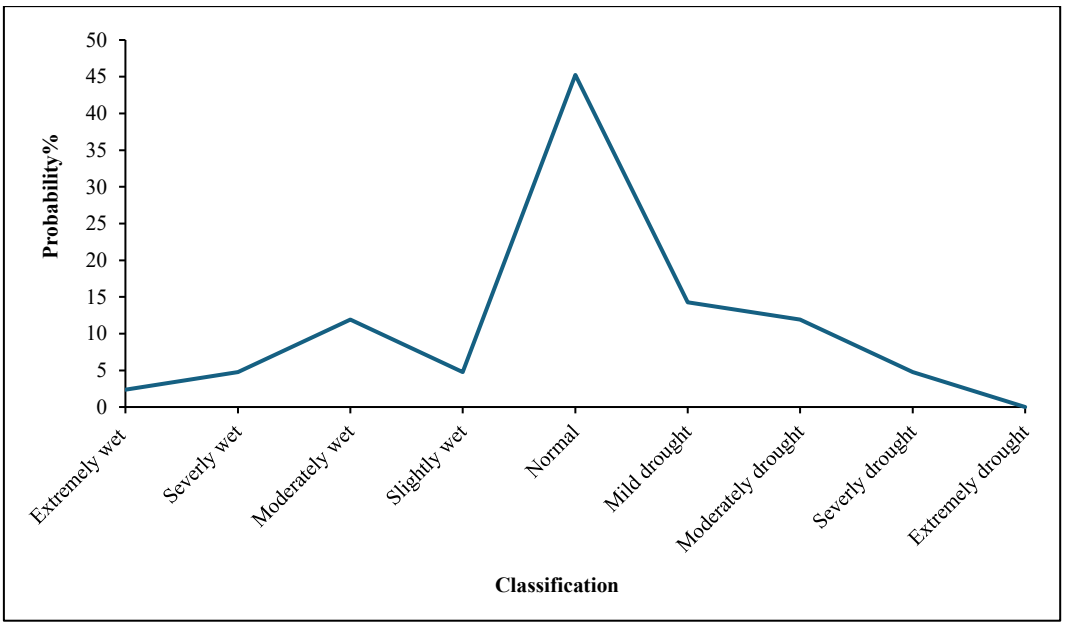

Figure 27. Probability of the annual SDI12 drought from 1980-2022

4. Conclusion

The Mann–Kendall and Sen's slope tests indicate a decline in the average annual rainfall trend by 0.15 over 32 years, primarily attributed to climate change, particularly in the final decade of the research, which experienced a significant reduction in rainfall. The designation of 2019 as a flood year followed several consecutive years of deficits, characterized by an average annual precipitation of 18.46 mm. Conversely, 2021 is considered the driest year, with an average precipitation of 2.76 mm, while the maximum and minimum temperatures showed a slight annual increase of 0.086°C and 0.066°C, respectively. The monthly trends of rainfall, Tmax and Tmin demonstrated a decrease in monthly rainfall throughout all months, except for April and October, which exhibited increases of 0.32 mm and 0.018 mm, respectively. July and August are the hottest months of the year, with maximum temperatures attaining 45.1°C in July 2017 and August 2003, and the minimum temperature recorded was -1.8°C in January 2008. The statistical examination of annual rainfall variability indicates that climate change caused unpredictable increases in rainfall throughout the periods of 1991 to 1998, 1999 to 2006, 2007 to 2014, and 2014 to 2022. The box-and-whisker analysis of monthly rainfall variability reveals that November and February displayed the most dispersion. From 1991 to 2022, the flow rate of the Euphrates River near Husibah village decreased by 41% due to the filling of the Ataturk Dam in Turkey from 1992 to 1995. Since 1996, it has become apparent that the Euphrates River has been impacted by climate change and is experiencing aridity, particularly in 2018; the preceding three hydrological years have been characterized by drought. The research illustrated the alterations in the flow regime of the Euphrates River over 32 years, employing the flow duration curve. The annual flow rate variability indicates a 10% probability of flows exceeding 850 m^3/s and a 90% probability of flows exceeding 251 m^3/s. The Euphrates River lacks the characteristics of a natural flow regime because of the hydraulic infrastructure that controls its flow. A correlation exists between climate components and the Euphrates flow rate, with a low correlation of -0.36 for temperature and 0.29 for rainfall. The data reveal that the decline in the Euphrates River's flow is mainly due to reduced water imports from upstream countries, which adversely affect both the quantity and quality of the water.

The SDI3 results indicate that the water year 1987–1988 was extremely wet within three months, especially from April to June, which was characterized by increasing precipitation and melting. A significant drought occurred from July to September in the water year 2014–2015 and from January to March in 2021–2022 due to a lack of rainfall and the transfer of water to the Euphrates River by upstream riparian countries. For SDI6 indicator data, the period from April to September of the water year 1987–1988 experienced extraordinary precipitation, whereas the period from October to March of 2021–2022 was characterized by a significant drought. The water year 1987–1988 is characterized by excessive precipitation from October to September, as indicated by the SDI12 findings. The water years 2014–2015 and 2021–2022 experienced significant drought. According to the results of the SDI3 indicator, it can be inferred that the drought period started in the 1983–1984 water year, attributed to the filling of the Keban Dam in Turkey as part of the GAP project and the Tabaqa Dam in Syria (1974-1977). This study's evaluations are reliable for hydrologists and water resource management experts to ensure optimal water management and meet the diverse needs of water users during wet, moderate, and dry years. The municipal, agricultural, and industrial sectors, together with marshland ecosystems, rely on the water discharged from the Haditha Dam into the Euphrates River, which is dependent on the water flow from upstream countries. Because Iraq is located downstream of the Euphrates River, the country must continue negotiations with upstream nations to ensure it receives an adequate quantity and quality of water from the river. Moreover, it is essential to deeply investigate the effect of climate change on the Euphrates and develop appropriate approaches for dealing with the water crisis, considering the rising need for water and global warming.

5. Declarations

5.1. Author Contributions

Conceptualization, Z.H. and S.K.; methodology, Z.H. and S.K.; software, Z.H.; validation, Z.H. and S.K.; formal analysis, Z.H.; investigation, Z.H. and S.K.; resources, Z.H.; data curation, Z.H.; writing—original draft preparation, Z.H. and S.K.; writing—review and editing, Z.H.; visualization, Z.H. and S.K.; supervision, S.K.; project administration, Z.H. and S.K. All authors have read and agreed to the published version of the manuscript.

5.2. Data Availability Statement

The data presented in this study are available in the article.

5.3. Funding

The authors received no financial support for the research, authorship, and/or publication of this article.

5.4. Conflicts of Interest

The authors declare no conflict of interest.

6. References

[1] de Waal, D., Khemani, S., Barone, A., & Borgomeo, E. (2023). The Economics of Water Scarcity in the Middle East and North Africa: Institutional Solutions. World Bank Group, Washington, United States. doi:10.1596/978-1-4648-1739-7.

[2] UN ESCWA. (2019). Moving towards water security in the Arab region. United Nations Economic and Social Commission for Western Asia, Beirut, Lebanon. Available online: https://www.unescwa.org/publications/moving-towards-water-security-arab-region (accessed on July 2025).

[3] Wehrey, F., Dargin, J., Mehdi, Z., Muasher, M., Yahya, M., Kayssi, I., ... & Yabi, G. (2023). Climate Change and Vulnerability in the Middle East: A Call for Inclusive Reforms. Carnegie Endowment for International Peace, Washington, United States.

[4] Al-Muhyi, A., Bashar, A. L. A. J., & Kwyes, A. (2016). The study of climate change using statistical analysis case steady temperature variation in Basra. International Journal of Academic Research, 3(2), 5.

[5] Arvind, G., Ashok Kumar, P., Girish Karthi, S., & Suribabu, C. R. (2017). Statistical Analysis of 30 Years Rainfall Data: A Case Study. IOP Conference Series: Earth and Environmental Science, 80, 012067. doi:10.1088/1755-1315/80/1/012067.

[6] Zaghloul, M. S., Ghaderpour, E., Dastour, H., Farjad, B., Gupta, A., Eum, H., Achari, G., & Hassan, Q. K. (2022). Long Term Trend Analysis of River Flow and Climate in Northern Canada. Hydrology, 9(11), 197. doi:10.3390/hydrology9110197.

[7] Rao, Gr., Sowjanya, A., Shekhar, D., Naik, Bns., & Kiran, B. (2023). Rainfall analysis over 31 years of Chintapalle, Visakhapatnam, High Altitude and Tribal zone, Andhra Pradesh, India. Mausam, 74(3), 685–698. doi:10.54302/mausam.v74i3.818.

[8] Minh, H. V. T., Lien, B. T. B., Hong Ngoc, D. T., Ty, T. Van, Ngan, N. V. C., Cong, N. P., Downes, N. K., Meraj, G., & Kumar, P. (2024). Understanding Rainfall Distribution Characteristics over the Vietnamese Mekong Delta: A Comparison between Coastal and Inland Localities. Atmosphere, 15(2), 217. doi:10.3390/atmos15020217.

[9] Muhammad, Z. H., & Obead, I. H. (2024). Quantifying Meteorological Drought Severity for the Watersheds in Euphrates River Basin, Central Euphrates District, Iraq. Iraqi Geological Journal, 57(1D), 240–256. doi:10.46717/igj.57.1D.18ms-2024-4-28.

[10] Leon, L. P., & Oculi, N. (2023). Evaluating Rainfall and Temperature Trends in the Small Island Developing State of St. Lucia Using Nonparametric Statistics and Soft Computing. World Environmental and Water Resources Congress 2023, 317–327. doi:10.1061/9780784484852.031.

[11] Abubakar, K., Abaje, I. B., & Tukur, R. (2024). Rainfall and Temperature Dynamics in the Context of Climate Change in the Sudan Savanna Ecological Zone of Katsina State, Nigeria. FUDMA Journal of Earth and Environmental Sciences, 1(2), 82–98. doi:10.33003/jees.2024.0102/08.

[12] WHO. (2025) Drought. World Health Organization (WHO), Geneva, Switzerland. Available online: https://www.who.int/health-topics/drought (accessed on July 2025).

[13] IPCC. (2023). Climate Change 2021 – The Physical Science Basis. Intergovernmental Panel on Climate Change (IPCC), Geneva, Switzerland. doi:10.1017/9781009157896.

[14] Wilhite, D. A., & Glantz, M. H. (2019). Understanding the drought phenomenon: The role of definitions. Planning for Drought: Toward A Reduction of Societal Vulnerability, 10(3), 11–27. doi:10.4324/9780429301735-2.

[15] UNDP. (2022). Institutional Survey & Assessment Report on Drought Early Warning System in Iraq. United Nations Development Programme, New York, United States. Available online: www.undp.org/iraq (accessed on September 2025).

[16] UNESCO. (2014). Integrated drought risk management, DRM: national framework for Iraq, an analysis report. United Nations Educational, Scientific and Cultural Organization (UNESCO), Paris, France.

[17] Shamout, M. N., & Lahn, G. (2015). The Euphrates in crisis: channels of cooperation for a threatened river. Chatham House for the Royal Institute of International Affairs, London, United Kingdom.

[18] World Bank Group. (2022). Iraq Country Climate and Development Report. World Bank, Washington, United States. doi:10.1596/38250.

[19] Nasir, H. N., & Hamdan, A. N. A. (2019). Drought Hazard Assessment in Iraq using SPI and GIS Systems. International Journal of Civil Engineering and Technology (IJCIET), 10(12), 161-173.

[20] Nedham, U. S., & Hassan, A. S. (2020). Comparison of Some Drought Indices in Iraq. Al-Mustansiriyah Journal of Science, 30(4), 1–9. doi:10.23851/mjs.v30i4.674.

[21] Tareke, K. A., & Awoke, A. G. (2022). Comparing surface water supply index and streamflow drought index for hydrological drought analysis in Ethiopia. Heliyon, 8(12), 12000. doi:10.1016/j.heliyon.2022.e12000.

[22] Dare, A., Zakka, E. J., Samson, M., Afolabi, A. O., Okechalu, S. O., & Amos, B. (2020). Drought Monitoring Using Rainfall, Evapotranspiration and Streamflow Data: A Case Study of Kaduna River Catchment Area (Nigeria). Journal of Scientific Research and Reports, 133–144. doi:10.9734/jsrr/2020/v26i830303.

[23] Al-Khafaji, M. S., & Al-Ameri, R. A. (2021). Evaluation of drought indices correlation for drought frequency analysis of the Mosul dam watershed. IOP Conference Series: Earth and Environmental Science, 779(1), 12077. doi:10.1088/1755-1315/779/1/012077.

[24] Al-Muhyi, ٍa. H., Aleedani, F. Y., Albattat, M. Q., & Badr, J. M. (2024). Rainfall Repercussions: Assessing Climate Change Influence on Iraq Precipitation Patterns. Al-Kitab Journal for Pure Sciences, 8(01), 92–103. doi:10.32441/kjps.08.01.p9.

[25] Dakhil, A. J., Hussain, E. K., & Aziz, F. F. (2024). Evaluation of the Drought Situation Using Remote Sensing Technology, an Applied Study on a Part of North Wasit Governorate in Iraq. Nature Environment and Pollution Technology, 23(4), 2241–2249. doi:10.46488/nept.2024.v23i04.028.

[26] da Silva, T. L., Romani, L. A. S., Evangelista, S. R. M., Datcu, M., & Massruhá, S. M. F. S. (2025). Drought Monitoring in the Agrotechnological Districts of the Semear Digital Center. Atmosphere, 16(4), 465. doi:10.3390/atmos16040465.

[27] Mann, H. B. (1945). Nonparametric Tests Against Trend. Econometrica, 13(3), 245. doi:10.2307/1907187.

[28] Hollander, M., Wolfe, D. A., & Chicken, E. (2013). Nonparametric statistical methods. John Wiley & Sons, Hoboken, United States.

[29] Gilbert, R. O. (1987). Statistical methods for environmental pollution monitoring. John Wiley & Sons, Hoboken, United States.

[30] Helsel, D. R., & Hirsch, R. M. (1993). Statistical methods in water resources. Elsevier, Amsterdam, Netherlands. doi:10.3133/tm4a3.

[31] Sen, P. K. (1968). Estimates of the Regression Coefficient Based on Kendall's Tau. Journal of the American Statistical Association, 63(324), 1379. doi:10.2307/2285891.

[32] Nalbantis, I., & Tsakiris, G. (2008). Assessment of Hydrological Drought Revisited. Water Resources Management, 23(5), 881–897. doi:10.1007/s11269-008-9305-1.

[33] Tukey, J. W. (1977). Exploratory data analysis. Addison-Wesley, Boston, United States.